Cruise Report

R.V. Poseidon **Cruise No.: 436**

Dates, Ports: 06.07.2012 (Kiel) – 31.07.2012 (Akureyri)

Research subject: North Kolbeinsey Ridge - geochemistry and volcanology

Chief Scientist: Prof. Dr. Colin W. Devey, GEOMAR, Kiel

Number of Scientists: 10

Project: Magmatism in the North Atlantic

The Scientific Team (left to right) Extreme back: Jan Mayen; Back: Momme Deutschmann, Evan Rivers, Colin Devey, Isobel Yeo, Nico Augustin, Froukje van der Zwan, Marcel Rothenbeck; Front row: Kelsey Meisenhelder, Lynne Elkins, Tea Laurila

Alphabetical List of Participating Scientists

Name	Affiliation
Augustin, Nico	GEOMAR, Kiel
Deutschmann, Momme	GEOMAR, Kiel
Devey, Colin	GEOMAR, Kiel
Elkins, Lynne	Bryn Mawr College, Philidelphia, PA, USA
Laurila, Tea	Univ. Ottawa, Canada
Meisenhelder, Kelsey	Bryn Mawr College, Philidelphia, PA, USA
Rivers, Evan	Bryn Mawr College, Philidelphia, PA, USA
Rothenbeck, Marcel	GEOMAR, Kiel
van der Zwan, Froukje	GEOMAR, Kiel
Yeo, Isobel	GEOMAR, Kiel

1 Introduction (Devey)

Although the magmas erupting at the global mid-ocean ridges are almost always tholeiitic, implying a globally common source mineralogy and melting regime, they show large variations in their trace element and isotopic compositions, presumably reflecting a fundamental heterogeneity of the Earth´s convecting upper mantle. Whilst some of this heterogeneity may be related to the interaction with nearby hotspots, large areas of the spreading axis are enriched in trace elements but show no nearby seamount chains. The enrichment on such ridges has been proposed to be the result of the presence of either localised blobs of enriched mantle or sublithospheric feeding of material over long distances from more distant hotspots - determining which of these is the correct cause can provide us with important knowledge about the heterogeneity of the Earth and global chemical cycles.

Determining the mineralogy and chemical nature of a mantle source is notoriously difficult, however, because of the trace element fractionation which occurs during melting. Only isotopic disequilibrium studies present the chance to determine true source characteristics, but these studies depend wholly on the availability of young (and, if possible, known age) samples. For very young submarine volcanic samples, the best time information is usually given by additional geological information from the sampling locations, allowing a relative stratigraphy and age scale to be determined.

One such shallow, enriched ridge segment whose geological and geochemical surroundings are particularly well characterized is Eggvin Bank on the northern Kolbeinsey Ridge. As part of a project involving researchers from GEOMAR, WHOI and Bryn Mawr College we used ships multibeam surveyed followed up by deep-diving AUV mapping to attempt to determine the location of the youngest volcanism on this ridge. A combination of holocene glaciation and high present-day sedimentation rates means that this ridge segment is highly suitable for distinguishing young volcanics, especially using the AUV side-scan sonar to identify sedimented and un-sedimented areas. The cruise provided a clear proof-of-principle for this type of stratigraphic work using an AUV and yielded some of the best-characterized mid-ocean ridge samples available anywhere on Earth. In the course of surveying and sampling work, the ridge axis was also thoroughly prospected for hydrothermal activity both by the AUV and by the use of MAPR attached to the sampling cable.

Acknowledgements

Our thanks to the Captain and crew of R.V. "Poseidon" for their excellent professional work throughout the cruise. Thanks also to Dr. E. Baker and his team at the NOAA Vents program for loan of the MAPR, and to the Norwegian and Danish (Greenland) authorities for permission to work in their EEZ.

2 The Geological Setting of the Northern Kolbeinsey Ridge (Devey, Elkins)

The Greenland basin initiated at 53-55 Ma with rifting between Greenland and Eurasia. Early rifting formed the Aegir, Jan Mayen, Mohns, and Gakkel Ridges [*Blichert-Toft et al.*, 2005; *Schilling et al.*, 1999] (for relevant locations, see Figure 2.1). After 10 Ma of rifting in this configuration, the north-propagating rift axis of the Kolbeinsey Ridge initiated to the west of Jan Mayen, simultaneous with continued Aegir Ridge spreading. The ridge jump to the Kolbeinsey Ridge concluded when rifting ceased on the Aegir Ridge around 26 Ma, trapping a fragment of continental lithospheric material extending south from Jan Mayen Island. The spreading direction of the Mohns Ridge changed from NNW-SSE to NW-SE at 25 Ma [*R. Mjelde et al.*, 2008].

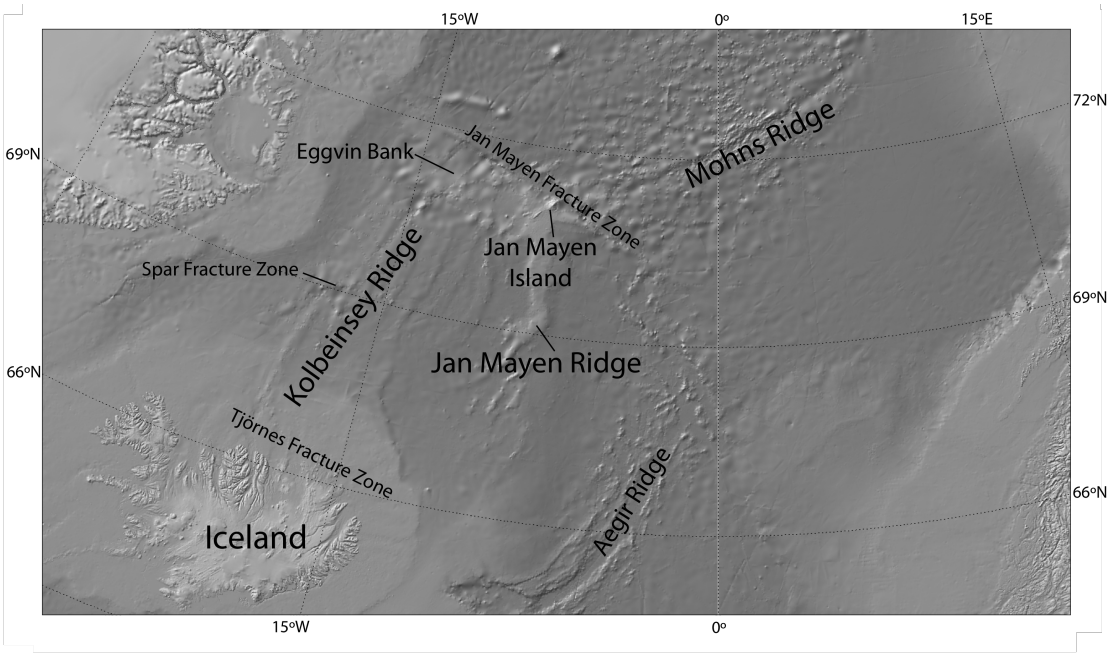

Figure 2.1: Map of study area, with features mentioned in the text labeled.

The modern Kolbeinsey Ridge is the slow-spreading (1.8 cm/yr. full spreading rate) segment of the Mid-Atlantic Ridge that initiates at Iceland on the leaky, overlapping Tjörnes Fracture Zone (66.8ºN) and extends north to the Jan Mayen Fracture Zone (71.5ºN). The Kolbeinsey Ridge has two non-transform offsets: the Spar overlapping zone at 69.1ºN and a second overlapper at 70.7ºN [*Haase et al.*, 2003]. The northernmost segment of the Ridge, north of 70.7ºN, is known bathymetrically as the Eggvin Bank and is characterized by anomalously shallow bathymetry [*Hooft et al.*, 2006]. Overall the Kolbeinsey Ridge overlies thick crust (7-10 km; [*Kodaira et al.*, 1997; *R. Mjelde et al.*, 2008]) and has an axial ridge depth that averages 1100 m; portions of the Kolbeinsey Ridge, however, are extremely shallow, including the southern portion immediately north of Iceland and the Eggvin Bank, which in off-axial places is only 40 m deep. Kolbeinsey Ridge spreading is nearly orthogonal to the orientation of the ridge axis, and the ridge is volcanically active along its entire length.

Kodaira [1997] suggested from morphologic observations and seismic measurements that the Jan Mayen Ridge, which lies adjacent to and East of the Eggvin Bank reflects the presence of rifted continental rocks, perhaps trapped by the ridge jump to the Kolbeinsey

Ridge at 25 Ma. More recently, Mjelde et al. [2009] have measured the seismic velocity structure of the Jan Mayen Ridge, confirming the likely presence of rifted continental material. The shallow bathymetry on the nearby Eggvin Bank ridge segment is to-date poorly explained and not well-mapped. Haase et al. [2003] suggested that the shallow bathymetry may result from the presence of an unusually buoyant mantle beneath the Eggvin Bank, creating a local bathymetric high, but the mechanism for emplacement of different mantle material west of the Jan Mayen Ridge remains unexplained. Mertz et al. [2004] have shown that young volcanism occurs at several places across the Bank but away from the spreading axis, suggesting that the mantle here is very fusible.

3 Cruise Narrative (Devey)

The cruise began in Kiel on 6th July with a slightly delayed departure to enable last-minute work on the software of the AUV in the hope of rectifying problems with the Reson multibeam. When both the AUV team and Reson technician were satisfied with the tests we departed Kiel for the trip through the Baltic and across the North Sea with course for the Jan Mayen Fracture zone. On the route we deployed 4 ARGOS floats for the international oceanography program. Due to occassional bad weather we arrived in the working area 7 days later, on 13.07 and made our first station to calibrate the MAPR and determine the water column temperature structure in an off-axis deep near the fracture zone. As even the position of the active spreading axis was poorly known on the Eggvin Bank region, we then commenced a zig-zag mapping course toward the SSW, aimed at determining the outline of the neovolcanic zone. After only 2 hours this course had to be interrupted due to the presence of drifting ice - unusual at this time of the year in this area. With patience and skill the officers managed to find routes through the ice patches to enable us to complete the mapping, however. This "dance with the ice" was a constant theme during the first few days in the working area, however, until a two-day period of strong winds from the NNE cleared the patches and their associated icebergs away

Figure 3.1: An iceberg over the North Kolbeinsey Ridge. Complicating but not stopping our research work.

A working rhythm established itself relatively quickly, with multibeam mapping to identify sampling and diving targets through the night hours interspersed with sampling (dredge and volcanic corer) and AUV stations during the day shift. The length of AUV dives varied according to target and sensor used between 10 and 24 hours. In some cases the shallow water near the axis allowed us to test a different type of AUV deployment, launching the AUV with sonar bottom contact and using transponderless dead-reckoning to navigate, with great success even for very long missions. During most of the working days calm weather greatly enhanced our efficiency and success, although the temperatures near 0°C made deck work cold and tiring for scientists and crew. The working program ended on 28.07 at 12:00 and the journey to Akureyri was begun. We arrived in Akureyri at 18:00 on 30.07.12 in time to clear customs and immigration and begin unloading and disassembling our scientific equipment.

4 Ship´s bathymetry (Augustin, Yeo)

4.1 Ship Based Multibeam

During RV Poseidon cruise P408 extensive multibeam mapping was carried out with a Seabeam 3050 echo sounder system provided by ELAC Nautik GmbH. The SeaBeam 3050 multibeam echo sounder collects bathymetric data in medium depth over a wide swath in excess of 140 degrees. The configuration installed at RV Poseidon operates in the 50 kHz frequency band in water depths ranging from 3 m below the transducers to approx. 3,000 m. It has an across-ship swath width of up to 140 degrees with up to 630 beams for each multi-ping (ELAC Nautik). Depending of the sea conditions we aquired good quality data in water depths up to 1700m (140-90° swath), while in deeper waters (below 2500m water depth) the sounding quality became to bad to resolve most features (50° swath).
The system consists of 2 transmitter/receiver units, a motion sensor, and a salinometer installed on the RV Poseidon. Data acquisition was carried out using the Hydrostar 3.5.8 software coupled with the survey and processing software package Hypack 11.0.1.49, running under Microsoft Windows XP (Figure 4.1). The Hysweep survey module of the bundle collected all data from the Seabeam echo sounder in its own HSX-data format. For deep-water sound velocity corrections we used MAPR profiles and AUV recorded water column data taken during P436.

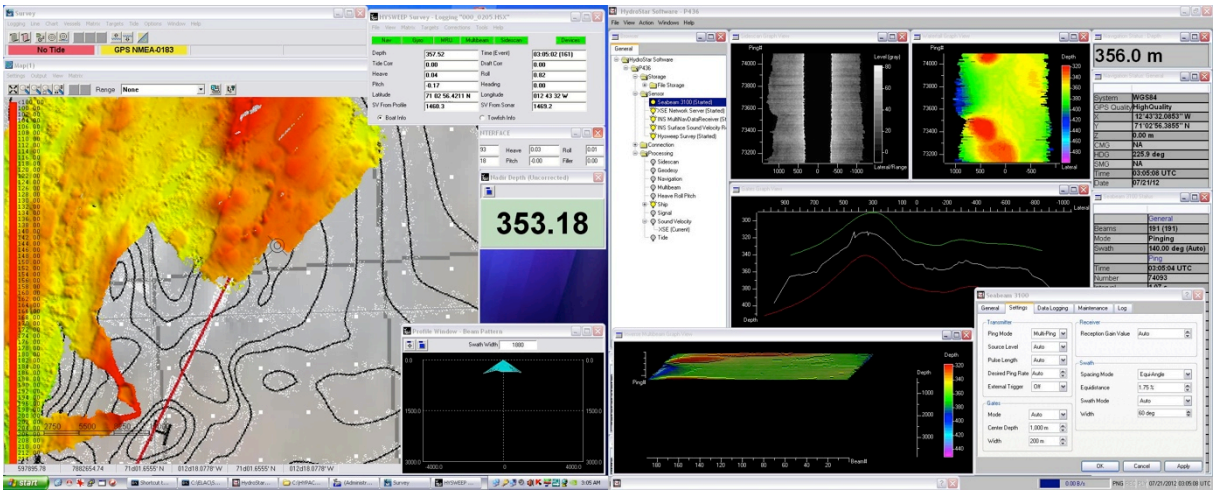

Figure 4.1: Hysweep Survey (Hypack, left) and Hydrostar (right) graphical user interfaces during mapping survey at the northern Kolbeinsey Ridge north of Mount Eggvin volcano (marked with "H" in the basemap left).

During P436 we collected a bathymetric dataset of approximately 3,130 km^2 along the eastern part of the northern Kolbeinsey Ridge (between 70.5°N and 71.7°N). The average ships speed during the bathymetric surveys was 6 knots.

The beam angle was mostly set to automatic mode in Hydrostar, but was manually corrected if necessary (e.g., because of less overlap of the mapped track lines). The Ping mode was set to Multi-Ping. Source Level, Pulse Length and Desired Ping Rate were set to Automatic. For bottom search the gates where first set manually and then switched to automatic mode after the bottom signal was found.

Preliminary data editing was done with the Hysweep Editor module (MBmax) including spike filtering and filtering of overhanging and underlying pings. Other available filter options (e.g.

quality filter) generated less effective or too strong beam filtering and were disabled. Accurate area based editing of selected parts for AUV mission planning was carried out using the 3DEditor modules included in the QPS Fledermaus Professional 7.3 software package.

Gridding and bathymetric map production was realized using the Fledermaus DMagic module and Global Mapper 13 (Fig. 2). Due to the data quality (dependant on water depth and weather conditions) the grid cell size was set variably between 10-35m. The preliminary maps were used for identifying geomorphological interesting structures (Fig. 3), sampling strategies and AUV mission planning.

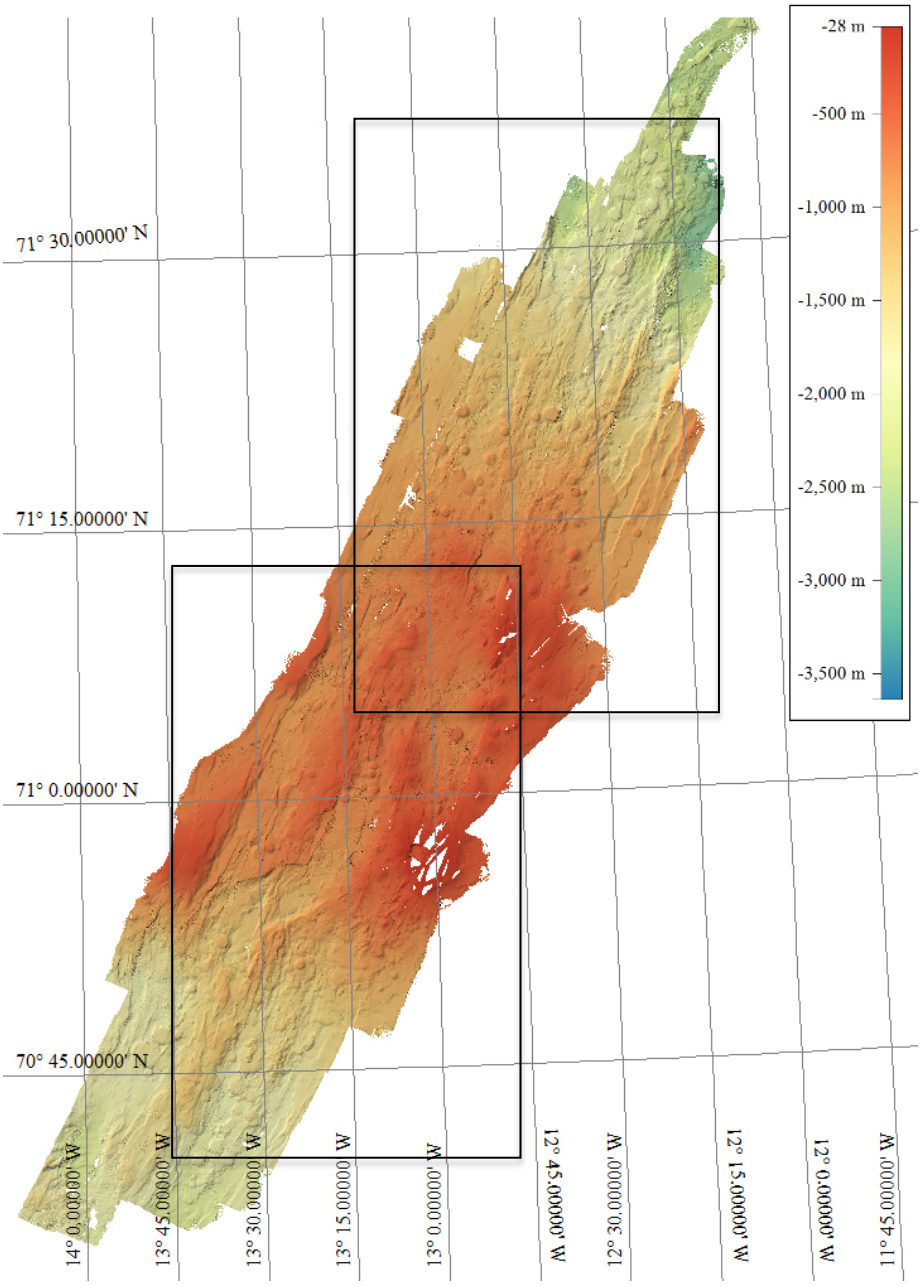

Figure 4.2: Preliminary processed bathymetric data of the working area. A total of about 3,100 km^2 with a north south extend of 140 km and an average width of 25 km. The boxes indicate the positions of detail maps in *Figure 4.3*

4.2 Technical Problems

Due to the different positions of all required sensors (e.g. motion, positioning etc.), to the sonar head, it is necessary to provide all offset information to the acquisition and post processing software in order for it to produce accurate bathymetric maps. Usually all necessary sensor offsets are written in a *.shipxse file for the use in Hydrostar and the so called Hypack- and Hysweep hardware drivers, which provide correction information to both programs for accurate calculation of the sounding position. During P436 we discovered that somehow these corrections in the multibeam software were wrong or not accurate, resulting in a horizontal position offset of up to 350 m between data obtained on different track lines. After consultation with ELAC we are still not certain of the cause of the problem, but were able to increase the data quality by performing several patch tests for pitch and latency. We found that a pitch offset was not responsible for the offsets but that a latency correction of -63.5 sec almost removed the discrepancy between the track lines (Figure 4.4). In general the ship based bathymetric maps also fit quite well to the AUV data (bathymetry as well as side scan data, Figure 4.5) after this correction. However, we found that in some places the position of prominent features still varies between different multibeam surveys (Figure 4.6) and that especially in shallow waters i.e., during the surveys of the summits of Mount Eggvin volcano (shallower that 100m) there were still clear offsets in the bathymetry, resulting in bumpy areas in the gridded files which made AUV dive planning highly inaccurate.
Even though the latency correction seemed to improve the positioning quality of large parts of the bathymetric data significantly, we are still unsure of the cause the offset problem. It is possible that a time stamp error in the RAW-Data files caused by latencies in the multibeam network, or the handshaking processes and data flow via the so called “shared memory” between Hydrostar and Hypack/Hysweep may also contribute to the problem. Random crashes of either Hypack/Hysweep or Hydrostar, the unexpected loss of Hysweeps connection to the sonar head may indicate some additional hard- or software problems, which could not be evaluated during the cruise. Detailed post processing of the collected data after the cruise should give additional information and help to repair any remaining errors.

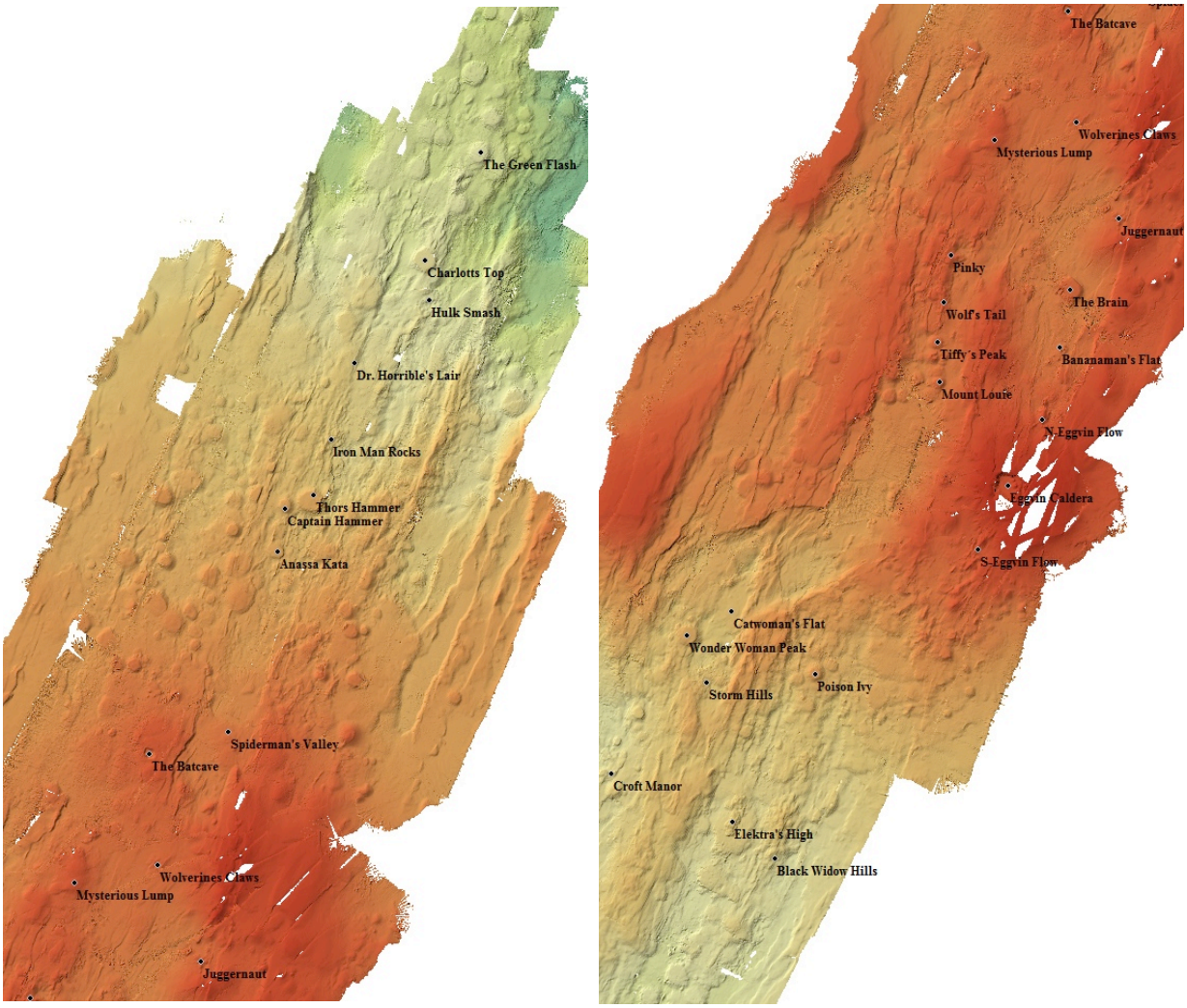

Figure 4.3: Details of the bathymetric map and overview of prominent features and sampling points discovered during P436 station works and AUV missions.

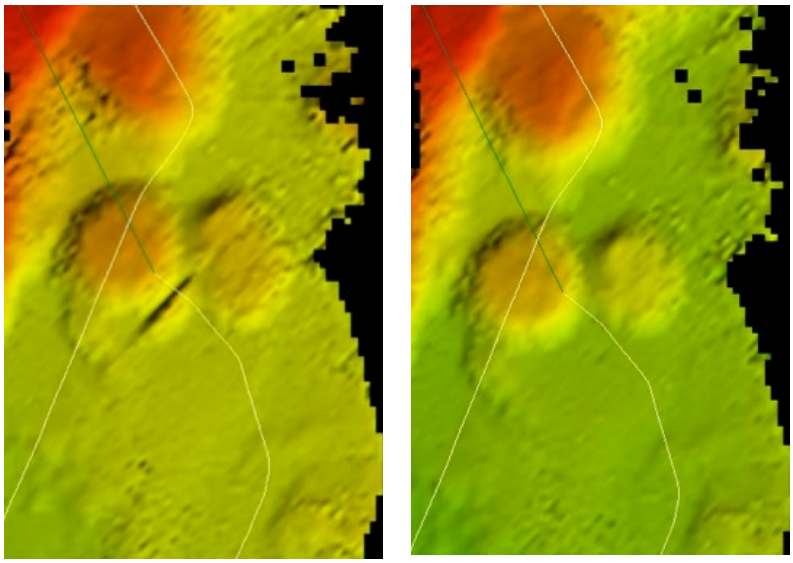

Figure 4.4: Two screenshots from the Hysweep Editor (MBMax) showing (left) an offset of about 350m of the SW flank of a flat top volcano at the end of a track line and (right) the same structure after using a latency correction factor of -63.5 sec. The white lines mark the nadir lines of the ship´s track.

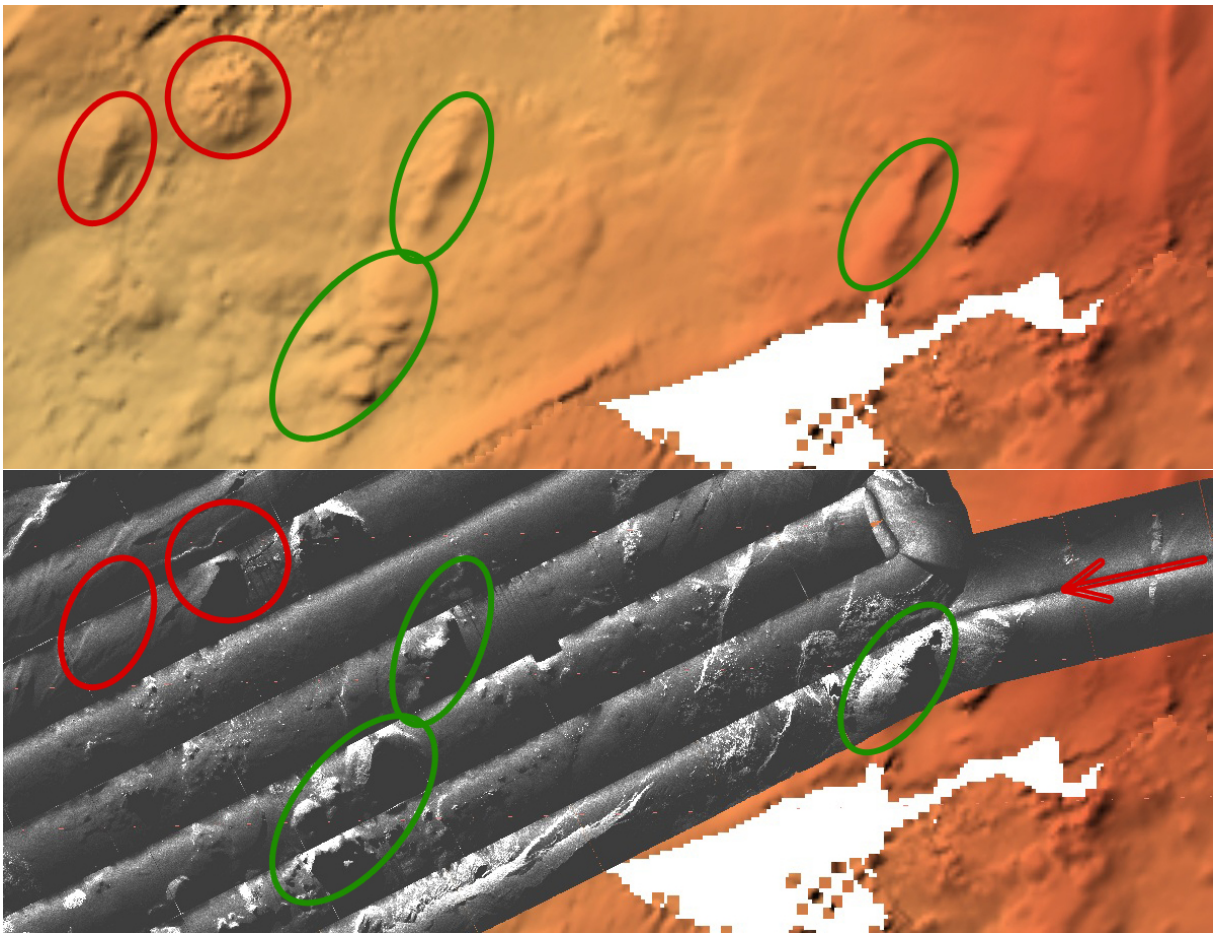

Figure 4.5: Comparison of ship based, latency corrected bathymetry (top) with AUV side scan sonar images (bottom) in screen grabs from Global Mapper. Small ridges and hummocky volcanics observed with the AUV fitting very well with related bathymetric structures (green ovals). Later in the mission the AUV data show a significant offset of about 400m in the position of the objects marked with red ovals. The red arrow indicates the beginning of the AUV mission; the geographic position of the colored ovals is in both pictures the same.

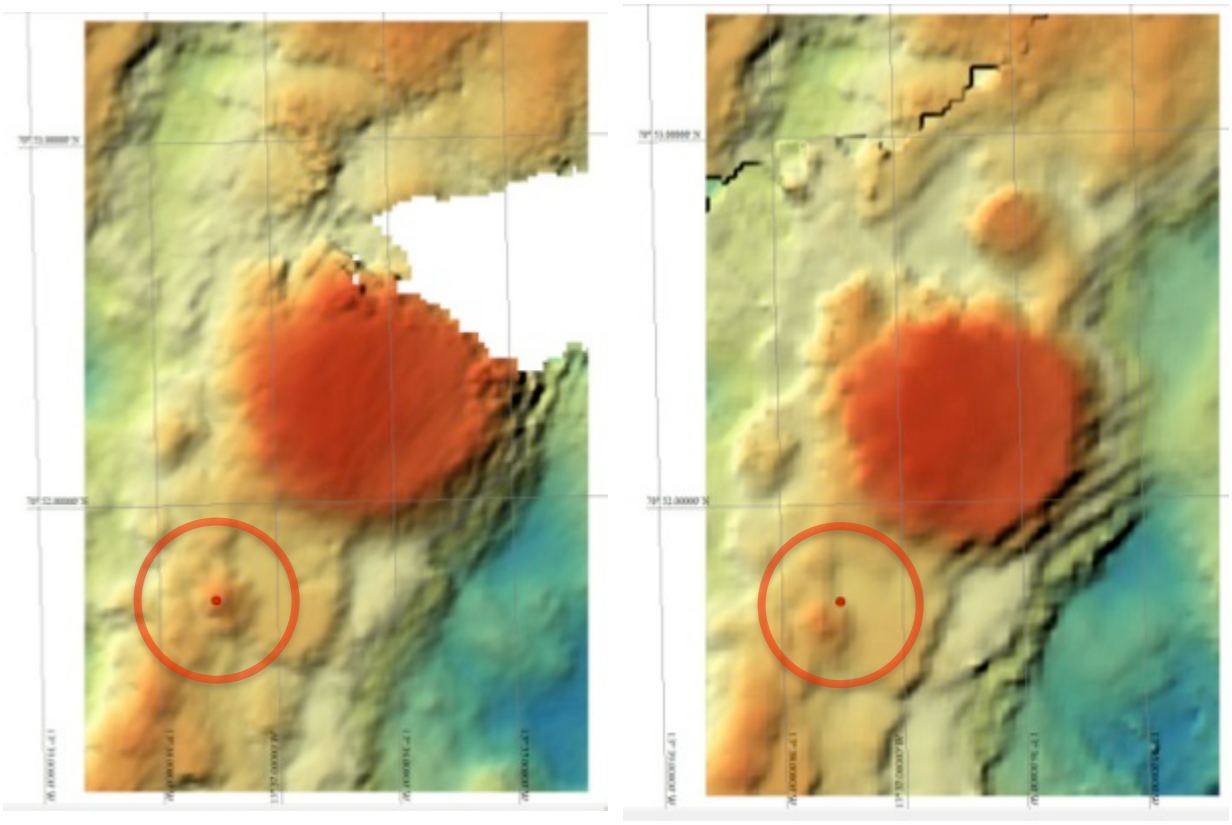

Figure 4.6: The maps show a mismatch between two different surveys oft he same area. The red point indicates the position of the top of a small mound SW oft he central flat-top volcano. In the right hand picture a second survey to close a data gap shows an offset in the position oft he same mound of about 150m to the SW (red point still shows the same geographic position). Both datasets were corrected with the same settings including the latency correction. The water depths are 1500-1140m.

4.3 Geological description of the Seabeam 3000 mapped area

The multibeam mapping of the North Kolbeinsey ridge segment reveals a complex pattern of volcanism and tectonics. At its northern end we image a single, 025° trending axial valley. The inner valley here is typically 4 – 5 km across, bounded by axis parallel normal faults, with throws mostly < 100m. These faults are separated from the main, > 100 m throw, stepped faulting complex both to the east and west by relatively flat (and probably heavily sedimented) plateaus, which extend for 3 – 4 km on both sides. This section of the ridge (north of 71°30 N) is characterized by predominantly flat-topped seamount volcanism, and at least 13 flat-topped seamounts can be observed, mostly within 1 – 2 km of each other. Those measured display typical height to diameter rations of ~ 1:10 [*Smith et al.*, 1995a; *Smith et al.*, 1995b].

Between 71°30 N and 71°00 N the ridge shallows dramatically to depths of > 500 m, mostly 200 – 300 m shallower than the rest of the ridge. The inner valley is similar to that observed further north (3 – 4 km) and is bounded by a few, small offset normal faults. Mostly the seafloor within the axial valley is fairly smooth looking, although a few rougher, possibly hummocky areas are observed, as well as a second zone of high-density flat-topped seamounts at ~ 71°20 N. The shallowest section of the ridge also displays a number of 1 – 2 km diameter low-lying irregular features, probably lava flows. The largest of these features (the 'Batcave') lies just west of the innermost western axial valley bounding fault, and is characterized by a large, 800m diameter crater. Some volcanic features can be observed

outside the inner valley here, notably at 71°04 N 012°50 W, where a large, 2km wide, high surrounded by an ellipse shaped depression is cut by the innermost large eastern axial valley wall fault, however most features appear smooth and lower relief than those within the valley, suggesting they are heavily sedimented.

At the southern end of this section, and just outside the axial valley to the east (at ~70°57 N 013°03 W) we image a large ~ 5 km diameter volcano (Eggvin volcano). The volcano is the tallest feature on the ridge and shallows to a depth of < 25 m at its summit. It lies directly on the intersection of the first large eastern axial valley wall fault and the southern bounding fault of the oblique valley (described in the next paragraph). The summit of the volcano is characterized by a ~ 2 km diameter caldera containing several small cones. Rougher areas on its southern flank may be recent volcanic eruptions.

South of ~ 71°00 N we image an oblique, normal fault bounded valley. The valley trends ~ 068° and extends for 7 km E – W. It is bounded at either end by further, axis parallel, normal faults. It also contains a central, axis parallel shallower zone of faulted terrain. The valley floor is mostly fairly flat, although some small areas of rougher terrain (which is probably volcanic) can be observed both east and west of the central tectonised zone. South of this valley the ridge is characterized by two parallel 25° striking valleys. The easternmost of the valleys sits in line with the axial valley further north, while the western valley lies 7 km to the west and connects with the western end of oblique valley. The valleys are separated by a shallower tectonised zone, approximately 4 km wide, containing both westerly and easterly dipping normal faults. Both valleys appear to contain volcanic edifices, the western valley mostly flat-topped seamounts and the eastern valley a combination of flat-topped seamounts, low lying flows and hummocky looking rough terrain. One hummocky flow in the eastern valley displays particularly sharp relief and is probably fairly unsedimented. No volcanic features are observed in the western valley south of 70°45 N, and this area of the valley is instead characterized by flat, smooth looking seafloor (although this could be volcanic). In contrast volcanic features are observed along the entire length of the eastern valley, although are dominated by relatively low relief flat-topped seamounts south of 70°45 N. Both valleys must have been volcanically active relatively recently, however from the Seabeam 3000 data it is impossibly to distinguish whether one, or both valleys are currently experiencing magmatic extension.

5 AUV Deployments (Rothenbeck, Deutschmann)

5.1 Technical description

The Autonomous Underwater Vehicle (AUV) ABYSS (built by HYDROID) from GEOMAR can be operated in water depth of up to 6000 m.

The ABYSS system comprises the AUV itself, a control and workshop container, and a mobile Launch and Recovery System (LARS) with a deployment frame that was installed at the stern of R/V Poseidon. The LARS was developed by WHOI to support ship-based operations so that no rubber boat is required to launch and recover the AUV. The LARS is mounted on steel plates which are screwed on the deck of the ship. The LARS is configured in a way that the AUV can also be deployed over the port or starboard side of the German medium- and large-size research vessels. The LARS is stored in a 20 ft. container during transport.

We can deploy and recover the AUV at weather conditions with a swell of up to 2.5 m and wind speeds of up to 6 beaufort. For the recovery the nose float pops off when triggered through an acoustic command. The float and the 20 m long recovery line drift away from the vehicle so that a grapnel hook can snag the line. The line is then connected to the LARS winch, and the vehicle is pulled up. Finally, the AUV is brought up on deck and safely secured in the LARS. During P436 only two recoveries had smaller challenges but the rubber boat was not used at all.

The vehicle consists of a tapered forward section, a cylindrical midsection and a tapered tail section. An internal titanium strongback, which extends through much of the vehicle length, provides the structural integrity and acts as a mounting platform for syntactic foam, equipment housings, sensors and release mechanisms. The maximum vehicle diameter is 0.66 meters and the overall length is 4 meters. Vehicle weight is approximately 880 kilograms, but is depending on the payload configuration. A rectangular compartment in the midsection of the vehicle contains three pressure housings and an oil-filled junction box. Two pressure housings each contain one 5.6 kWh 29-Volt lithium-ion battery pack. The third pressure housing contains the vehicle and sidescan sonar electronics. The vehicle's inertial measurement unit and acoustic Doppler current profiler are housed in two other independent housings that are mounted forward of the 3 main pressure housings. The propulsion and control systems are located in the tail assembly, which is bolted to the aft face of the vehicle strongback. The tail assembly consists of a pressure housing with motor controller electronics and an oil-compensated motor housing. Propulsion is generated with a 24 VDC brushless motor driving a two-bladed propeller. Control is achieved with horizontal and vertical fins driven by another 24 VDC brushless gear motors. The vehicle velocity range is 1.2 to 2.0 m/s, although best control is achieved at velocities above 1.5 m/s. The AUV descents with about 0.9 m/s whereas the ascent speed is about 0.5 m/s or 1m/s if the ascent weight is dropped. Together with the deployment/recovery procedure the descent to the seafloor and the ascent back to the vessel take approximately 2.5 hours at a water depth of 3000 m.

Sensors of the base vehicle include pressure, temperature, conductivity, optical backscatter, Edgetech Dual frequency (120/410 kHz) Sidescan Sonar and Eh-sensor (in cooperation with Dr. Koichi Nakamura, Japan); and an inertial navigation system that is aided by an Acoustic Doppler Current Profiler (ADCP) with bottom lock capabilities. In addition, the vehicle can be

reconfigured for three different modes of operation as follows

1. Base vehicle plus RESON Seabat 7125 Multi-Beam (200/400 kHz), or

2. Base vehicle plus Electronic Still Camera & Strobe not used during P436), or

3. Base vehicle plus Sub-Bottom Profiler (not used during P436).

5.2 AUV mission summaries

Dive 99 - 14.07.2012

Mission start: 19:49 UTC Mission time: 13.5 hours
Bottom time: 13.25 hours
Used sensors: Reson Seabat Multibeam 400 kHz , Eh sensor, Seabird SBE49 CTD, WetLabs ECO
Altitude / Line spacing: 50 m / 100 m
Distance travelled: 75.2 km
Coverage per hour: 0.6 km^2/h (in total 7.7 km^2)

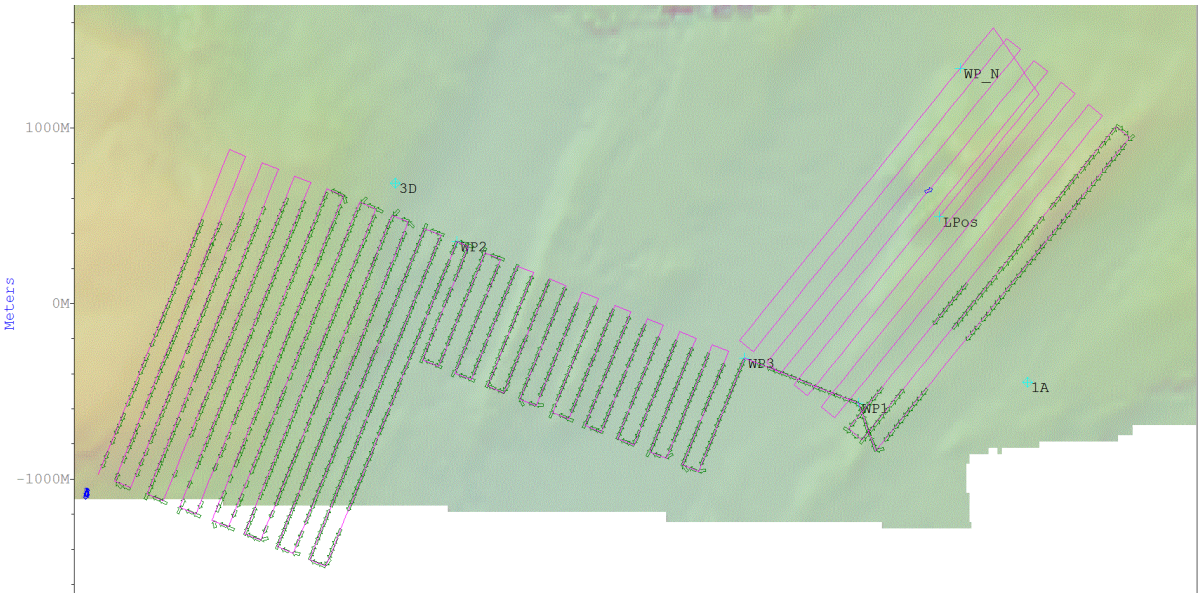

LBL coverage (long baseline) in mission 99 (green arrow - transponder fix)

Mission 99 was supposed to map two areas in high resolution bathymetry that are connected by a smaller 'mowing the lawn' pattern. Two transponders were positioned in a way to achieve continuous LBL coverage. The mission passed off without incident except the end since it stopped deep. This happened because of a missing command in the mission file that gives the order to come up to the surface.

Dive 100 - 16.07.2012

Mission start: 15:08 UTC Mission time: 15.4 hours
Bottom time: 14.8 hours
Used sensors: Reson Seabat Multibeam 400 kHz , Eh sensor, Seabird SBE49 CTD, WetLabs ECO
Altitude / Line spacing: 50 m / 100 m
Distance travelled: 84.8 km
Coverage per hour: 0.6 km^2/h (8,3 km^2)

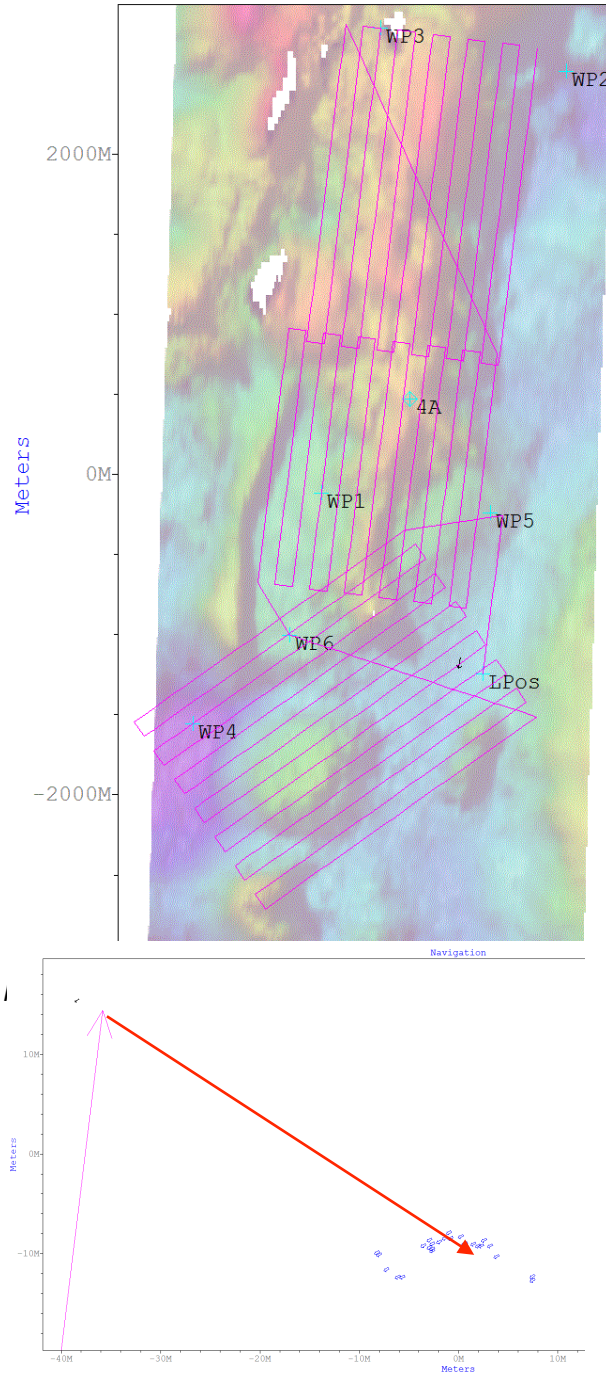

Position offset at mission end

Mission 100 used the RESON multibeam. Again two transponder were set to provide position update but they were not used because of a wrong setting in the mission file. Nevertheless the navigation error was unexpectedly low according the processed multibeam data (100% overlap). The GPS position update at the end of the mission showed a position offset of only 40 meters. The vehicle dived through 500 meters water column and travelled almost 15 hours above the sea floor with a very small navigation error. There was a general position offset because of the descent phase through the water column but the overlapping data points do match. These good results without position updates from the LBL transponders means a very good dead reckoning caused by the support of the ADCP (Teledyne RDI Workhorse Navigator). By neglecting the descent phase a navigation error of app. 2.6 meters per hour could be achieved without an INS.

Dive 101 - 18.07.2012

Mission start: 05:27 UTC Mission time: 09.28 hours
Bottom time: 08.22 hours
Used sensors: Reson Seabat Multibeam 400 kHz , Eh sensor, Seabird SBE49 CTD, WetLabs ECO
Depth / Line spacing: 1070 m / 100 m (above the flat top volcano)
Altitude / Line spacing: 50 m / 100 m (above the northern ridge)
Distance travelled: 51.5 km
Coverage per hour: 0.5 km^2/h (3.7 km^2)

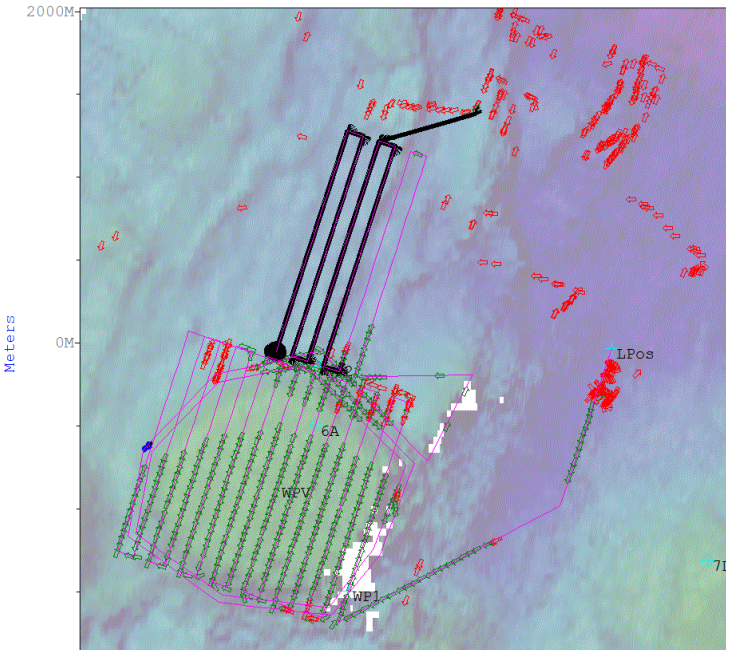

Mission track with used (green) and unused (red) LBL fixes

Mission 101 was suppose to map a flat top volcano in detail and its northern foothill. The transponder had to be set on one side of this formation. The vehicle got good fixes in the southern mission area on top of the volcano. In the northern part the fixes became more seldom and wrong fixes dominated. These initially not used fixed were caused by multipath ranges since the eastern transponder could not been seen by the vehicle. Finally one of these wrong fixes was accepted by the vehicle navigation at the third last leg and that caused a huge jump of the navigation of more than 500 meters. The vehicle corrected its position to the apparent position soon afterwards. In reality the vehicle changed its position to the southwest and finished the mission with an offset.

Dive 102 - 19.07.2012

Mission start: 04:42 UTC Mission time: 13.8 hours
Bottom time: 13.1 hours
Used sensors: Edgetech Sidescn 120 kHz , Eh sensor, Seabird SBE49 CTD, WetLabs ECO (Turbidity)
Altitude / Line spacing: 50 m / 700 m
Distance travelled: 74.2 km
Coverage per hour: 3.9 km^2/h (51.5 km^2)

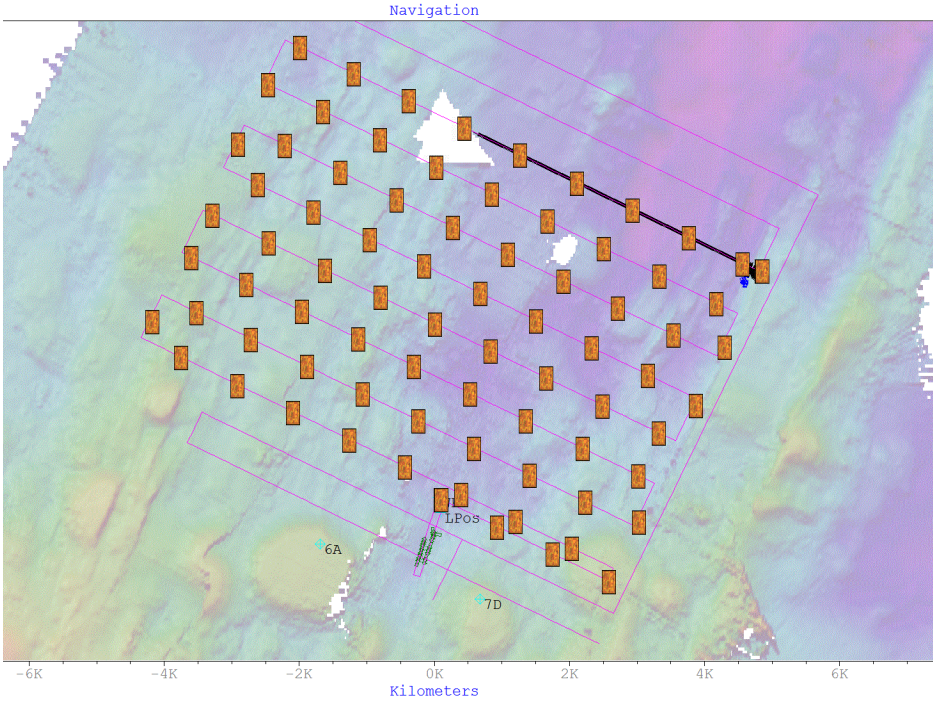

Planned mission with Sidescan files and LBL fixes

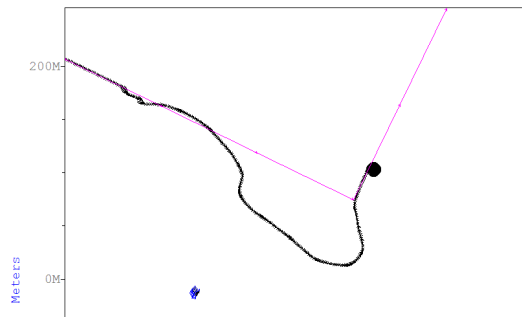

Abort with released recovery float

Mission 102´s goal was to get "big picture" view of this part of the ridge valley. The same transponders as dive 101 were used, although the vehicle was only allowed to get fixes during the first legs to avoid multipath ranges. The line spacing of 700 meters gave maximum coverage and avoided holes in the sidescan mosaic (30% overlap). At the end of one of northern legs the vehicle had bottom contact and soon afterwards it released the recovery float off its nose. According to the logged fault messages it executed a command from the digital transponder board that usually is sent from the ship based system. The mission was aborted by a timeout since it got the rope of the recovery float in the propeller and the speed was reduced to zero. The vehicle recovery proceeded better than expected since the deck crew could untangle the rope by using boat hooks.

Dive 103 - 21.07.2012

Mission start: 04:55 UTC Mission time: 23.2 hours
Bottom time: 22.2 hours
Used sensors: Edgetech Sidescan 120 kHz, Eh sensor, Seabird SBE49 CTD, WetLabs ECO (Turbidity)
Altitude / Line spacing: 50 m / 500 m
Distance travelled: 129.3 km
Coverage per hour: 2.9 km^2/h (64.4 km^2)

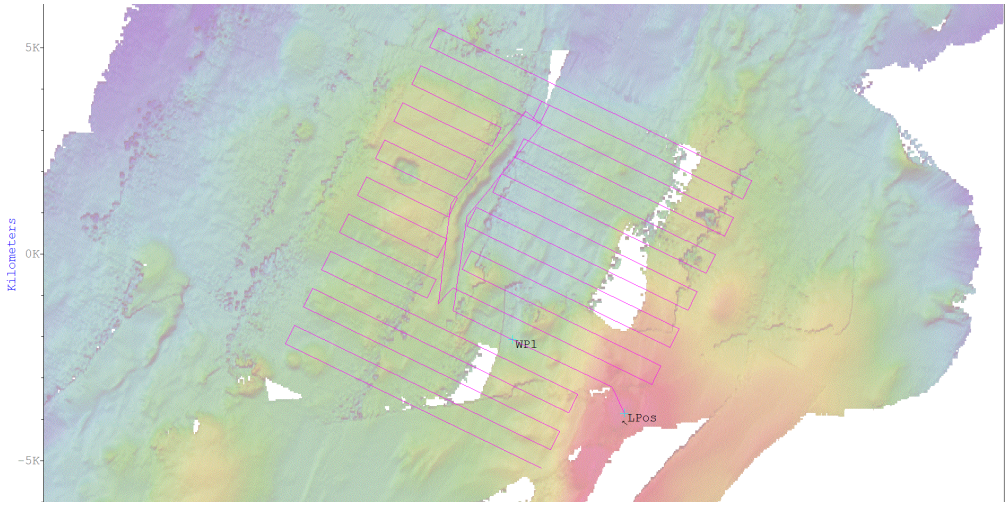

Planned mission

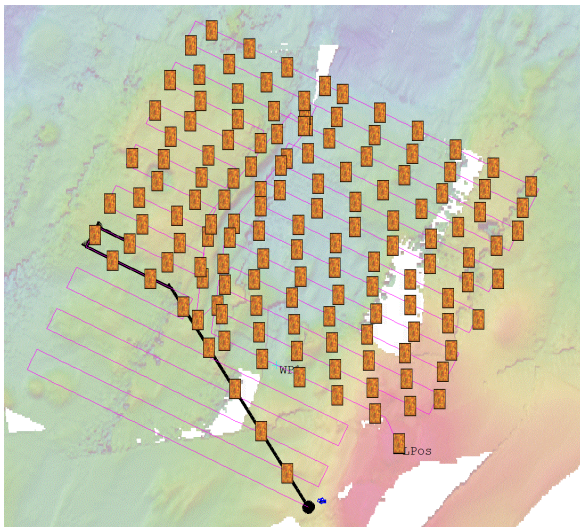

Logged sidescan files during mission 103

Mission 103 was also aimed at a bigger picture of the spreading axis. It was the second sidescan mission. The line spacing was set to 500 (100 % overlap) meters to get a continuous mosaic illuminated from one side. The mission started in a shallow area so the vehicle had bottom lock at launch so transponders were not used. The legs of the 'mowing the lawn' pattern were orientated across the axis of the valley to reduce bigger shadows in the sidescan mosaic. The mission time was planned for full capacity, based on results from mission 102. Mission 103 terminated when battery capacity reached the limit of 5% and the vehicle headed to the end position to abort there. The vehicle dropped the weight and came up.
The continuous low water temperature seemed to reduce the power consumption of the vehicle consumers. Even by using the multibeam configuration we could achieve mission lengths of more than 130 km (23 hours). It seemed to be caused by the lower consumption because the lithium ion battery cells need higher temperatures to come into their best capacity zone.

Dive 104 - 23.07.2012

Mission start: 14:53 UTC Mission time: 23.6 hours
Bottom time: 22.7 hours
Used sensors: Edgetech Sidescan 120 kHz, Eh sensor, Seabird SBE49 CTD, WetLabs ECO (Turbidity)
Altitude / Line spacing: 50 m / 500 m
Distance travelled: 129.3 km
Coverage per hour: 3.2 km^2/h (71.9 km^2)

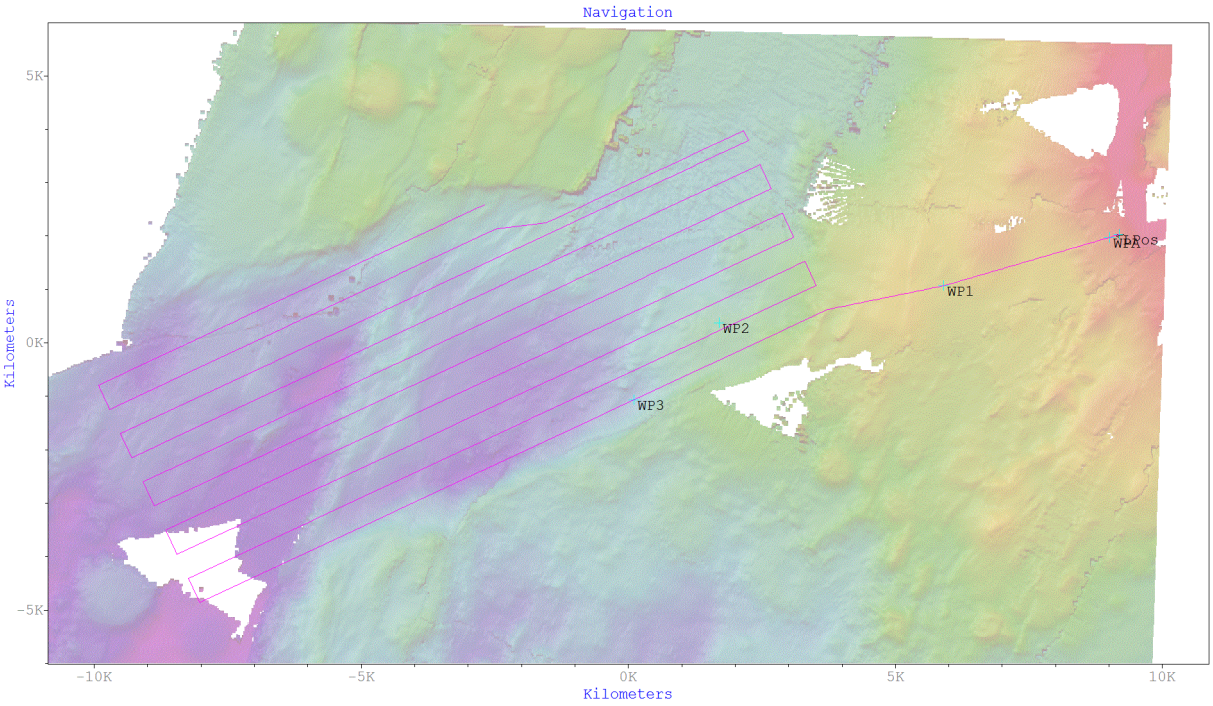

Planned mission

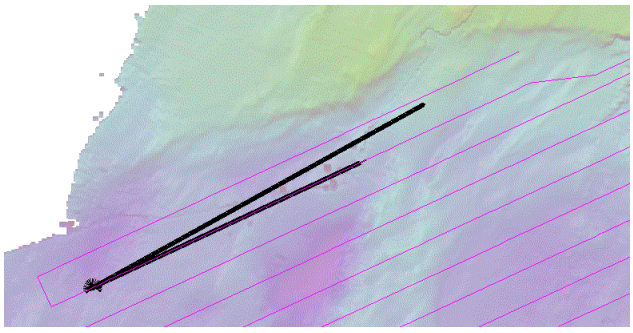

Software shut down on the way to end position

The start of mission 104 was set above the south western flank of the Eggvin volcano. The vehicle had bottom lock as soon as it was launched. This mission was programmed without transponder due to the good ADCP supported dead reckoning during the previous missions. The legs of the 'mowing the lawn' pattern were orientated along the axis of the valley to reduce bottom contacts. The mission time was planned according mission 103. The mission was stopped at the end of the leg before the last one and the vehicle headed to the end position to abort there. Underway the voltage reached the limit and the vehicle software was shut down by the emergency board. The vehicle dropped the weight and came up. The recovery float was release by acoustic commands.

Dive 105 - 25.07.2012

Mission start: 08:26 UTC Mission time: 10.8 hours
Bottom time: 10.12 hours
Used sensors: Edgetech Sidescan 120 kHz, Eh sensor, Seabird SBE49 CTD, WetLabs ECO (Turbidity)
Altitude / Line spacing: 50 m / 500 m
Distance travelled: 59.5 km
Coverage per hour: 2.9 km^2/h (28.9 km^2)

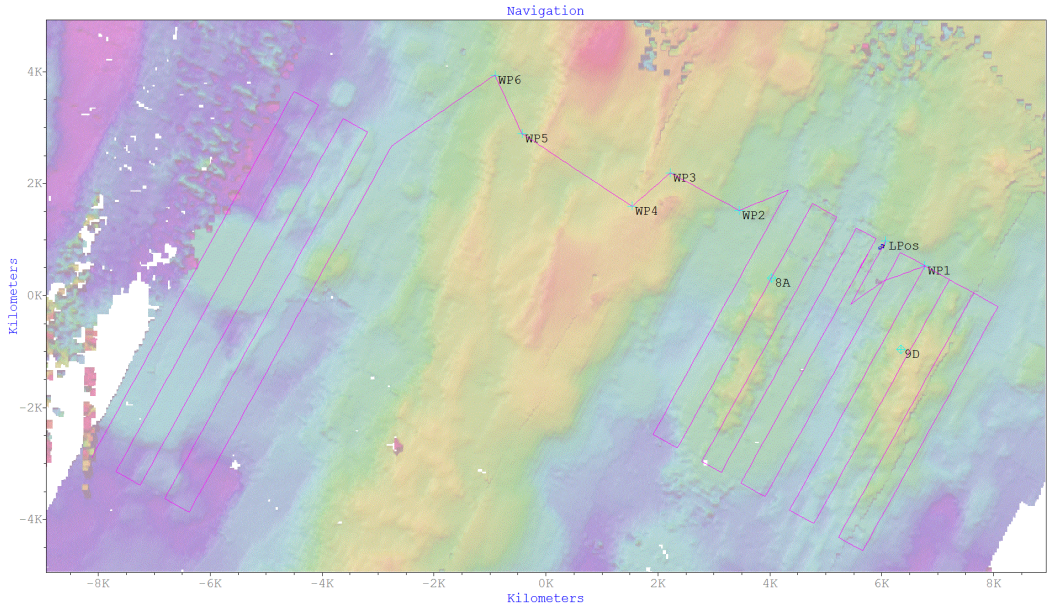

Planned mission

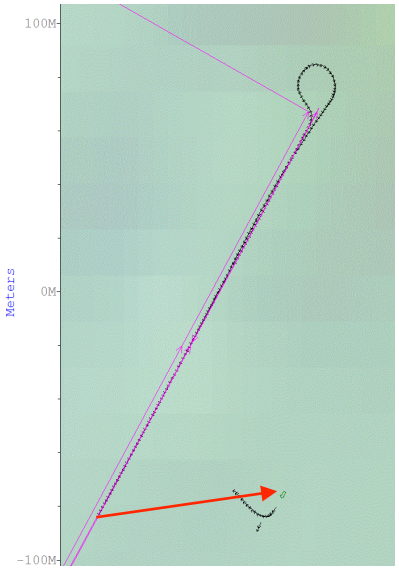

Position offset

Mission 105 was supposed to map two areas separated by a ridge. The transponders 8A and 9D were set in a way to support the vehicle with position fixes just after it reached the seafloor and in between the two survey patterns. All the other mission legs were programmed for dead reckoning navigation. The second LBL navigation phase was reached after more than six hours and 37km and it led to a shift of 70 m. During the following legs the navigation was as well supported by the INS (Inertial Navigation System) even though they were programmed as dead reckon objectives. This indicates good navigation fixes since the INS must be convinced of a consistent navigation. The exact transponder position update led to this good result additionally.

Because of an unforeseen abort only the eastern part of this mission could be almost completed. The mission abort was caused by a leak indication in the tail section following a bottom contact. Although this normally should lead to ascent weight being dropped, mud and glass in the ascent weight bay blocked this.

Dive 106 - 26.07.2012

Mission start: 14:58 UTC Mission time: 2.13 hours

Bottom time: 1,48 hours

Used sensors: Edgetech Sidescan 120 kHz, Eh sensor, Seabird SBE49 CTD, WetLabs ECO (Turbidity)

Altitude / Line spacing: 50 m / 500 m (for the undone western pattern)

Distance travelled: 12.1 km

Coverage per hour: 5.7 km^2/h (8.4 km^2)

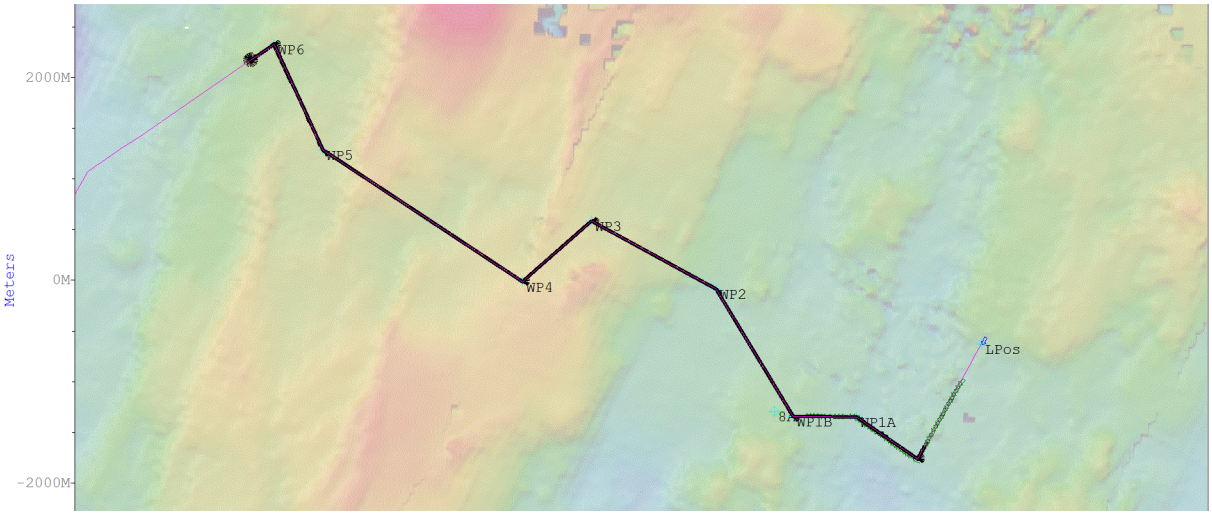

Distance travelled (black line)

Mission 106 was supposed to map the undone western area of mission 105 and the connection between both areas. The vehicle started on the same position as the previous one and got good fixes on its first legs. All the following legs were programmed in dead reckoning. Mission 106 had the same settings (altitude, line spacing etc.). The vehicle had no bottom contact. Just after waypoint 6 again a leak in the tail section of the vehicle was reported (fault message log). The ascent weight could be released this time. The vehicle came up and sent status messages via Iridium.

The RV Poseidon was being in the northern part of the main working area while the vehicle surfaced. It was decided to let it drift during the night because of the working program and the good weather situation. The vehicle was recovered without any issues in the morning of the following day.

Dive 107 - 27.07.2012

Mission start: 19:05 UTC Mission time: 11.9 hours
Bottom time: 11.4 hours
Used sensors: Edgetech Sidescan 120 kHz, Eh sensor, Seabird SBE49 CTD, WetLabs ECO (Turbidity)
Altitude / Line spacing: 50 m / 500 m
Distance travelled: 65.7 km
Coverage per hours: 3.8 km^2/h (43.0 km^2)

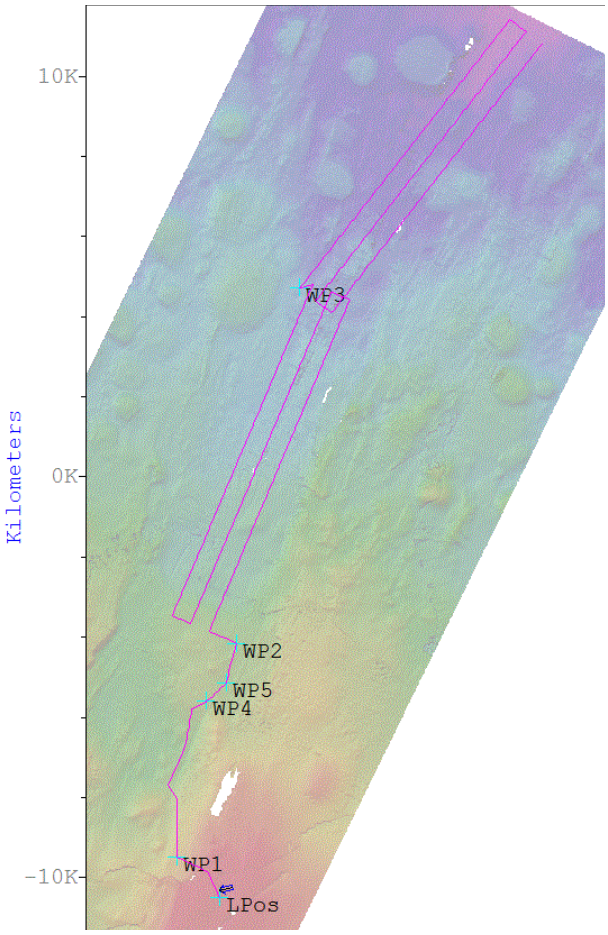

Planned mission

The last mission of cruise P436 was to get a connection between the mapped areas of dive 102 and 103. It was planned as a overnight mission. The transponder were again not set because of the shallow part of the ridge what was supposed to be the launch position.
Mission 107 was successful and was not aborted due to the leak message of the tail probe.
The sidescan logged in total 73 JSF files. The processed data show too many faults in the sidescan mosaic. Probably this issue was caused by skipped sidescan circles as the vehicle log file shows. The exact reason of both the disturbed sidescan and the single leak message has to be verified.

6 AUV Seafloor Imaging results (Yeo)

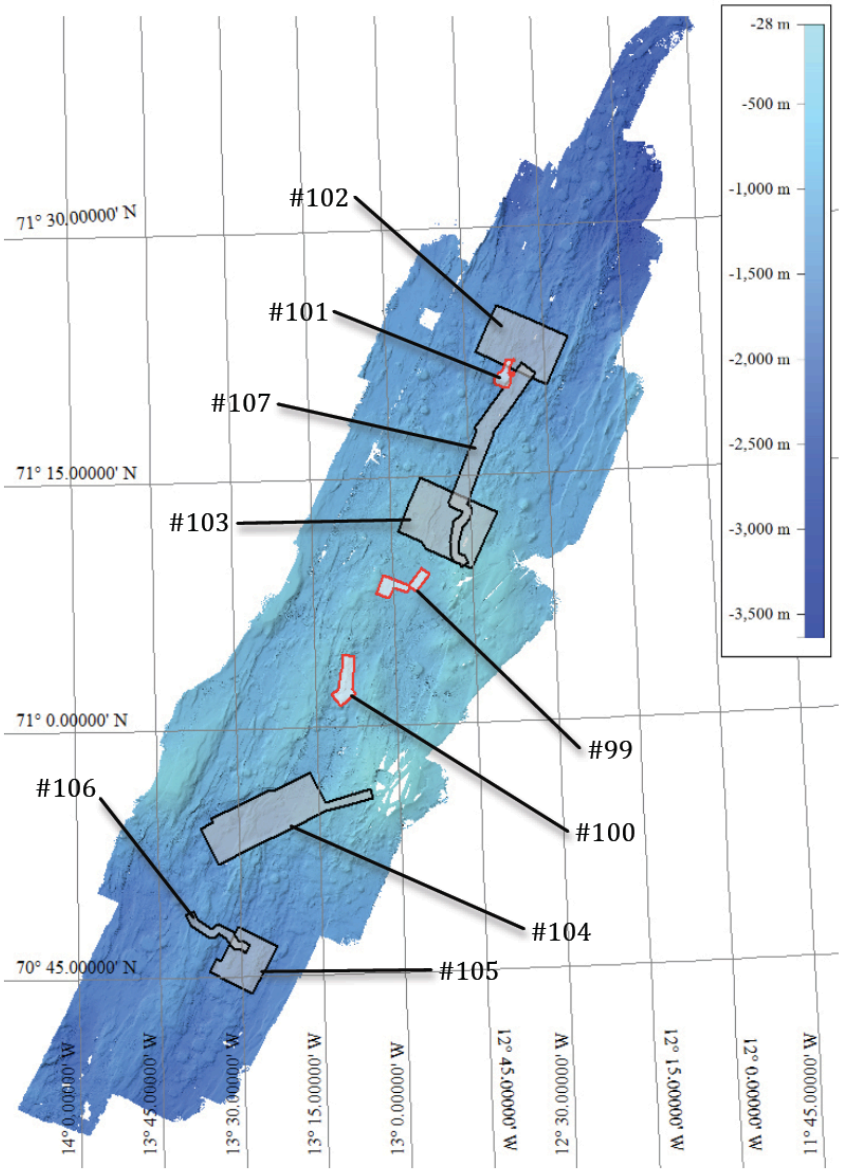

Figure 6.1: Overview of AUV mission areas during P436. Red outlines mark AUV multibeam surveys, black rimed areas display side scan sonar missions. For more details see text.

6.1 AUV Multibeam

The AUV mounted RESON Seabat 7125 multibeam system (200/400 kHz) was used during three AUV dives at P436 (Figure 6.1). We operated the system at 400 kHz with 512 equi-angular beams. Besides the mandatory data such as sonar settings, beam geometry data and bathymetric data we also recorded backscatter imagery data and snippets, which are needed for processing the backscatter data (because of their amplitude information). A single transmission from the projector unit illuminates a 128° swath on the sea floor. The seabed return signal is received by the receiver unit, digitized, and stored as *.S7K files, a proprietary RESON format, on a hard drive. The amount of data increases by approximately 10 MB per minute during a high frequency survey. This rate depends of course on the ping rate. The multibeam surveys are operated in altitude mode (50m), meaning the vehicle is following the

topography as closely as possible. The ping rate was set to automatic mode and varies with the altitude. In general, the dive missions were planned using a line spacing of 100m with an overlap of approximately 20%. A new file is created for every 256 MByte of data collected. The bathymetric data collected with the AUV have been quality checked, preliminary processed and gridded with RESONs PDS2000 software with a spatial acoustic resolution up to 1m.

6.2 AUV Side Scan Sonar

Six missions were accomplished during P436 by using the Edgetech 2200-MP sidescan sonar 120/410 kHz (Figure 6.1). The 120 kHz surveys recorded high definition data from a total area of about 270 km^2. In general, a side-scan survey is planned in altitude mode (50m above the seafloor) where the vehicle follows the topography. The line spacing of a sidescan pattern differs from the multibeam in two ways. Firstly, the line spacing is wider due to the wider range. Thus, the resulting swath width provides coverage of about 2 km² per hour. In addition, the line spacing is chosen to provide 100 % overlap, making it possible to produce two sidescan maps with opposite illuminations. In our case we chose a line spacing of 500 meters. The side-scan data are acquired in form of *.JSF files and processed initially with the software SonarWiz 5.04.

6.3 First Results of AUV Surveys

6.3.1 Abyss #099 (Multibeam Survey, 7.7 km2)

Survey objectives: The earliest Seabeam 3000 mapping conducted showed a small area of axis parallel ridges at 71°08.96 N 012°54.60 W, sitting close to the axis defined from crustal magnetization (Applegate, pers. comm.). These ridges were separated from a smooth, rounder high at 71°08.53 N 013°02.04 W by an area of flat seafloor. With limited Seabeam mapping completed, this area provided the opportunity to test the hypothesized location of the axis, while also examining the nature of three different landforms.

Geological description: The survey revealed the three ridges to be eastward facing normal faults. Scarp dips vary from 80° on the innermost fault to 30° on the ridge furthest from the axis, suggesting that back tilting of fault blocks is occurring away from the ridge. No volcanic morphology can be discerned on or around the fault blocks and sediment flow structures can be observed off the southern end of the fault blocks, suggesting that sediment thicknesses here must be upwards of several meters.

Between the ridges and the smooth high the dive covers an area of flat seafloor. Some structure can be observed in the flat seafloor, although it has a relief of < 5 m and is not identifiable as either volcanic or sedimentary. The very smooth surface texture suggests sediment thicknesses of > 1 m. The flat seafloor is cut by two further ~ 30 m high, westward dipping (~ 50°) faults.

The smooth high shows the most surface texture of the survey, displaying some 40 – 60 m wide, 10 – 20 m high hummocky edifices, although their low relief suggests they are also heavily sedimented. The top of the high lies 120 m above the flat seafloor at its base, but is smooth, relatively flat (< 5° sloping) and probably heavily sedimented.

6.3.2 Abyss #100 (Multibeam, 8.32 km^2)

Survey objectives: Survey area 0100 was designed to cover a 3 km long by 0.7 km wide ridge at 71°03.38 N 013°09.07 W and a 640 m wide flat-topped seamount at 71°01.68 N 013°09.80 W to the south. Both hummocky ridges and flat-topped seamounts are common mid-ocean ridge volcanic edifices, and both the seamount ad the ridge appeared to have sharper relief than the surrounding seafloor, suggesting they were younger. Additionally, the hummocky ridge appeared to postdate pre-existing fault, which it cuts across.

Geological description: The survey imaged both the hummocky ridge (Figure 6.2) and the flat-topped seamount south of it. The ridge itself appears to be composed of 30-100 m diameter, <50 m high hummocks on its flanks, but is characterized by a fairly flat, 100-250 m wide summit area. This summit area is devoid of features and is probably sedimented. The ridge itself is probably not very young, showing some evidence of sediment draping (lack of definition between hummocks and gentle, smooth slopes). Additionally the ridge is cut by a small eastward dipping fault, with a 5 m offset. This fault (as well as the axial valley wall fault) also cuts a roughly circular, 570 m diameter, flat-topped edifice west of the ridge, which may be an old flat-topped seamount.

The summit of the flat-topped seamount shows some detail, suggesting that sediment thicknesses are <2-3 m. The highest point is at 71°01.64 N 013°09.89 W, slightly south and west of its centre. It has a height of ~150 m, giving it a height to diameter ration of ~1:10, typical of flat-topped seamounts elsewhere [*Smith et al.*, 1995a; *Smith et al.*, 1995b]. The flanks are steep (slope angles of up to ~80°), and show some scalloping on the northern side, as well as a more gently sloping apron around the base, suggesting mass wasting. Probably due to sedimentation, individual flow fronts cannot be recognized on the summit.

The seafloor between the seamount and the ridge is deeper, but characterized by small hummocks. Areas of smooth seafloor can also be seen south and west of the ridge and seamount at 71°01.83 N 013°11.17 W. No detail can be discerned from the survey, but given the typical relief of the hummocks and their proximity to the ridge axis, they are probably low relief lava flows. North of the ridge at least 5 small ridge parallel faults can be seen, some of which appear to cut an area of lower relief, probably older hummocky seafloor. The ridge itself sits on a flat region of slightly shallower seafloor, which is truncated at it's southern end by an ~E–W orientated scarp, probably as a result mass wasting, which could represent an earlier phase of flat-topped seamount volcanism.

The survey also images a section of the innermost western axial valley wall fault. The fault dips eastward with an angle of ~70°, is roughly ridge parallel and has a throw of 44 m.

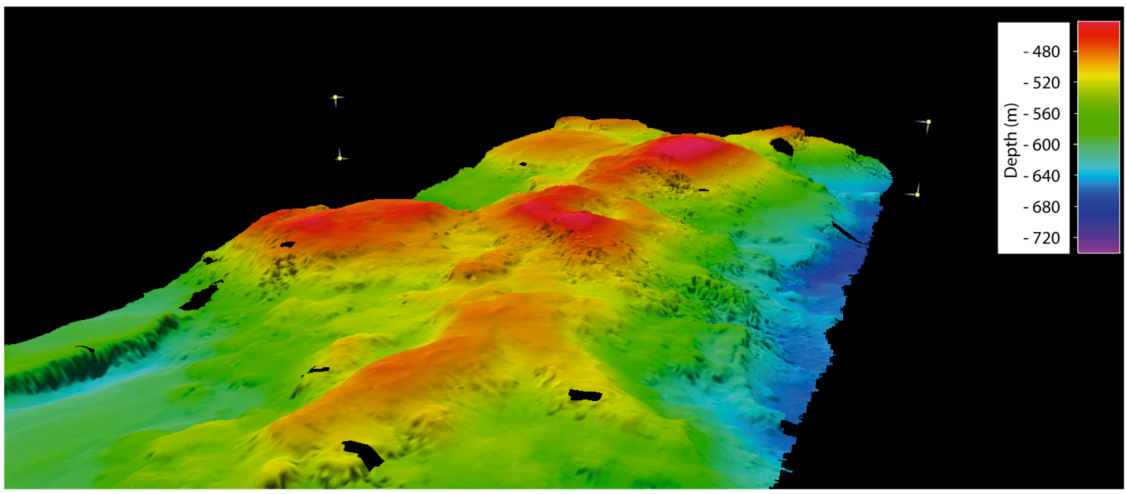

Figure 6.2: The hummocky ridge covered by survey Abyss #100. The field of view is ~ 1.5 km wide, looking NNW. Note the flat, smooth top of the ridge in contrast to its hummocks flanks.

6.3.3 Abyss #101 (Multibeam, 3.8 km^2)

Survey objectives: The 1.3 km wide flat-topped seamount at 71°20.83 N 012°37.75 W (Thor´s Hammer) is a typical example of the flat-top dominated volcanism observed on section of the ridge, particularly north of 71°15 N. Modes of formation of flat-topped seamounts are still not fully understood, in particular whether they are mono or polygenetic features. The sharp relief of the seamount and the sharp breaks in slope observed between the seafloor and its base in profile suggested relatively low degrees of sedimentation, and the seamount also cross cuts at least one underlying structure. A detailed survey of a young flat-topped seamount, particularly the summit, not only allows for identification of different lave flows, but also makes it possible to directly target individual flows and features with the rock corer.

Geological description: The survey images a 110 m high seamount with 60° slope flanks and a height to diameter ration of 1:11. The base of the flanks are characterized by a more shallowly dipping apron composed in places of smooth sediment or talus and in other areas of <50 m diameter, <20 m high hummocks. The highest point is at 71°20.80 N 012°37.71 W roughly in the centre of the summit. This summit area (Fig. 9) is characterized by rough, angular blocks ~50 m across, which are probably broken blocks of sheet flow. Other sheet flow textures, such as tumuli and skylights can be seen all over the summit.

At least two roughly concentric zones of increasing depth can be observed radiating out from the summit. Each one drops by 2–3 m and they may represent different flows from a central vent. The summit is also characterized by at least 5, roughly N–S orientated fissures, some of which are surrounded by slightly raised areas, which are commonly bounded by the fissure on one side. These areas may either represent smaller volume lava flows erupting from these fissures, or the fissures may simply produce relief that controls the flow of lava across the summit.

North of the seamount an elongated area of hummocky terrain is also imaged. The hummocks are orientated roughly axis parallel, however their connection to the seamount is unclear as a navigational jump obscured the bathymetry in this area. With further processing of the data this relationship should become clear.

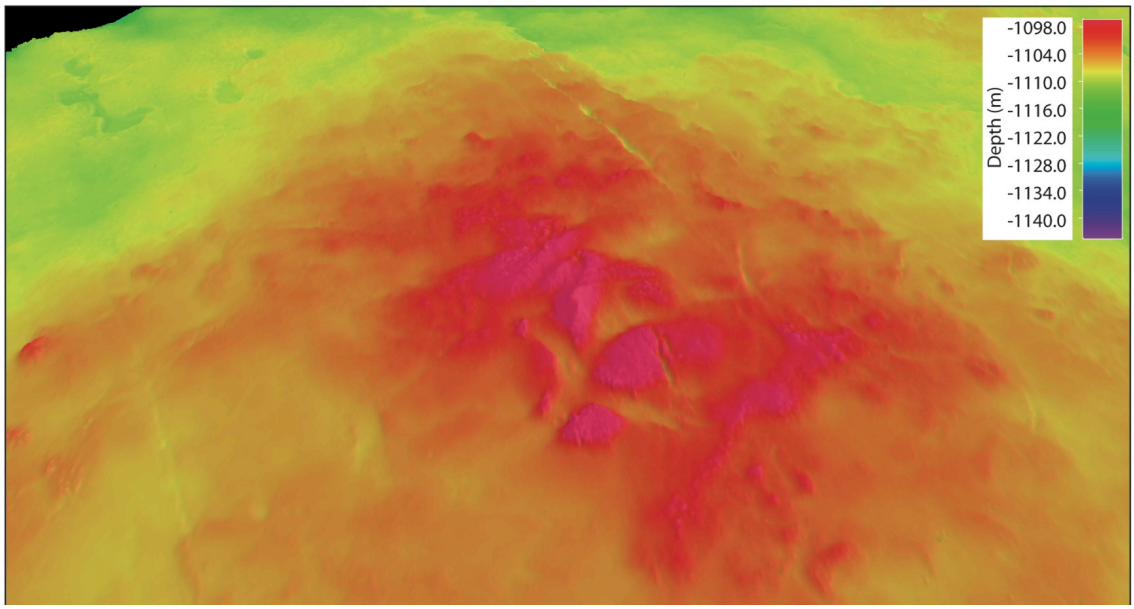

Figure 6.3: View (looking southwest) of AUV multibeam (Abyss #101) across the summit of the flat-topped seamount Thor´s Hammer . Field of view is ~800 m. The summit of the volcano (centre) is composed of blocky sheet flow lavas and is cross cut by a roughly N–S trending fissure (upper centre). Breaks in slope may represent flow front. Examples of drain out collapse pits can also be seen (upper left).

6.3.4 Abyss #102 (Sidescan Sonar, 51.5 km^2)

Survey objectives: Having acquired detailed multibeam of the three major terrains observed in the Seabeam 3000 bathymetry, sidescan sonar surveys made it possible to distinguish between these different terrains across a larger area. Area #102 was chosen to cover a high relief hummocky looking ridge at 71°22.82 N 012°35.45 W, just north of the seamount covered by survey #101. The survey was designed to cover this flow, and to provide high-resolution coverage of an entire E–W section of the axial valley inner floor (as picked from the Seabeam 3000 bathymetry).

Geological description: The sidescan survey reveals a 3.2 km wide axial valley, filled with both hummocky and higher effusion rate lobate and sheet flows. The inner valley is bounded to the east and west by several small and one larger normal fault on both sides. These faults separate the brightly back scattering inner valley from less bright, more sedimented flanks.

Within the axial valley the hummocky ridge observed in the Seabeam bathymetry corresponds to an area of 50–100 m diameter hummocks, which sometimes coalesce into larger, composite hummocky edifices. In the hummocky areas there is a hummock density of ~100 hummocks per km^2. In the north east of the survey area a large (3.4 km^2) sheet flow meets the base of the hummocky terrain. The flow surface displays flow lobes, skylights and tumuli. The contact relationship is unclear, however the sheet flow is slightly less brightly backscattering than the surrounding hummocky terrain, suggesting it could be older. Other smaller areas of sheet flow can be observed between the hummocky flows. Small <30 m diameter hummocks can be seen on the summits of some of the larger hummocks.

Outside the axial valley old, poorly backscattering hummocks are observed in the west and both old hummocks and sheet flows in the east.

6.3.5 Abyss #103 (Sidescan Sonar, 64.4 km^2)

Survey objectives: Between 71°13 N and 70°58 N the Northern Kolbeinsey Ridge shallows by 200-300 m. This shallower section is also marked by a reduction in the number of flat-topped seamounts observed on the seafloor. The shallower depth is indicative of thicker crust and therefore requires volcanism to be taking place, probably at a higher rate than in the shallower northern or southern parts of the ridge. Survey #103 covers a second E–W section across the axial valley inner floor, across this shallower section of the ridge and allows for comparison of the style and extent of volcanism in this shallower area with that in the north.

Geological description: The sidescan survey reveals a 3.4 km wide volcanically active zone, filled with relatively brightly back scattering volcanics in the north of the area and covered by flat, poorly backscattering sedimented terrain in the south. It is bounded on both sides by one or more normal faults.

A much larger proportion of the lava flows in this area are flat sheet and lobate flows, characterized by flow lobes, skylights and tumuli (Figure 6.4). They cover at least 6 km^2 of the 14 km^2 of brightly backscattering volcanics in the inner valley. Hummocks are also common (Figure 6.5), although do not coalesce into such large topographic highs as in the north.

Outside the inner valley to the west the seafloor is dominated by sedimented sheet and lobate flows in the south and sedimented old volcanic hummocks in the north. The hummocks look very similar to those observed in the axial valley and elsewhere on the segment. However, while the sheet flows also display flow lobes, skylights and tumuli, the area of sheet flows is characterized by a 560 m wide crater (The Batcave, see also Figure 4.3) and a second round cratered edifice ~1 km south east of the crater (Figure 6.6). This edifice displays blocky sheet flows on its sides and appears to have fed a lava flow through its eastern side. Outside the eastern fault the seafloor is more poorly backscattering than on the east and is probably more heavily sedimented, however some texture indicative of sheet and lobate flows can be seen.

6.3.6 Abyss #104 (Sidescan Sonar, 71.9 km^2)

Survey objectives: At approximately 70°57 N the rift valley appears to deviate from the ~025° strike typical further north. An oblique valley, containing a roughly N–S orientated, shallower tectonised area is observed, striking ~68°. This offset zone may offset the main rift by up to 7 km. To see a ridge offset taking the form of a valley is unusual and very few such features have been documented. Survey #104 covers the floor of this oblique rift zone in order to assess whether the ridge has been offset or not, and whether there is any volcanism in the valley itself.

Geological description: The survey shows that most of the seafloor in area #104 is covered by poorly backscattering, however at least 10 km^2 of the survey area is covered by three bright, young looking sheet flows (Figure 6.7). The sheet flows display tumuli (possibly marking vents) and appear to grade into more hummocky, presumably pillowed, terrain at their distal ends.

As expected the slightly shallower tectonised region that cross cuts the valley is produced by a number of small faults, most of which dip to the west. Two of the sheet flows lie west of this area and one (the least brightly backscattering of the three) lies to the east. Other

regions of poorly backscattering, low relief, old hummocky terrain can be observed on both sides.

The western end of the valley is imaged, comprising several small and one large easterly dipping fault. The lower flanks of the large volcano at 70°56.87 N 13°03.29 are also covered by a single swath which illuminates at least 4 small easterly facing faults cutting through relatively poorly backscattering rough looking volcanic terrain, which is probably composed of pillow lavas.

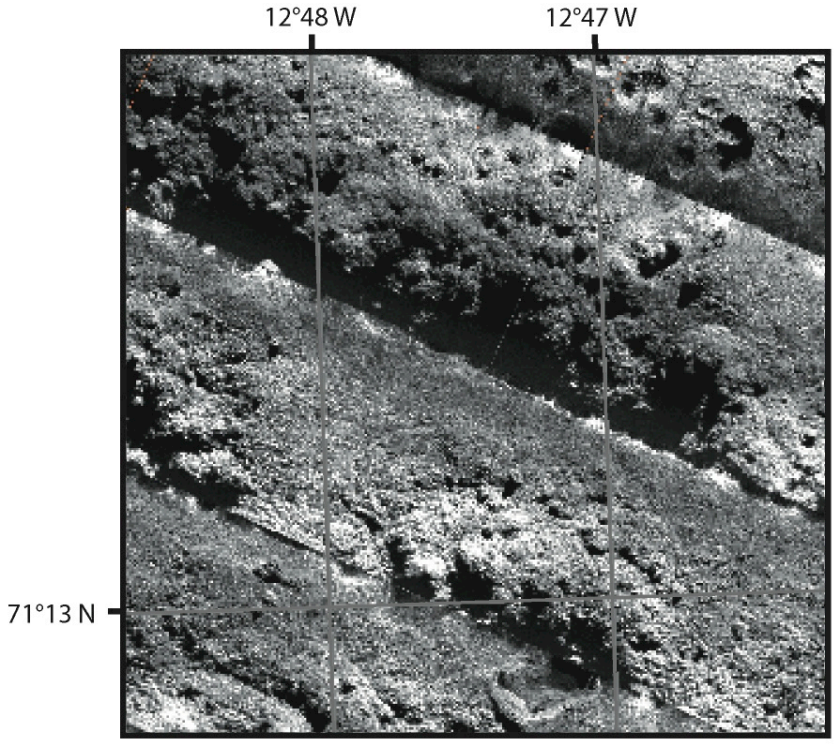

Figure 6.4: Sidescan sonar from Abyss #103 showing brightly backscattering young (southern half) and less brightly backscattering old (northern half) hummocky terrain. Sheet flow texture can be seen on the surface of the flow at the bottom of the picture.

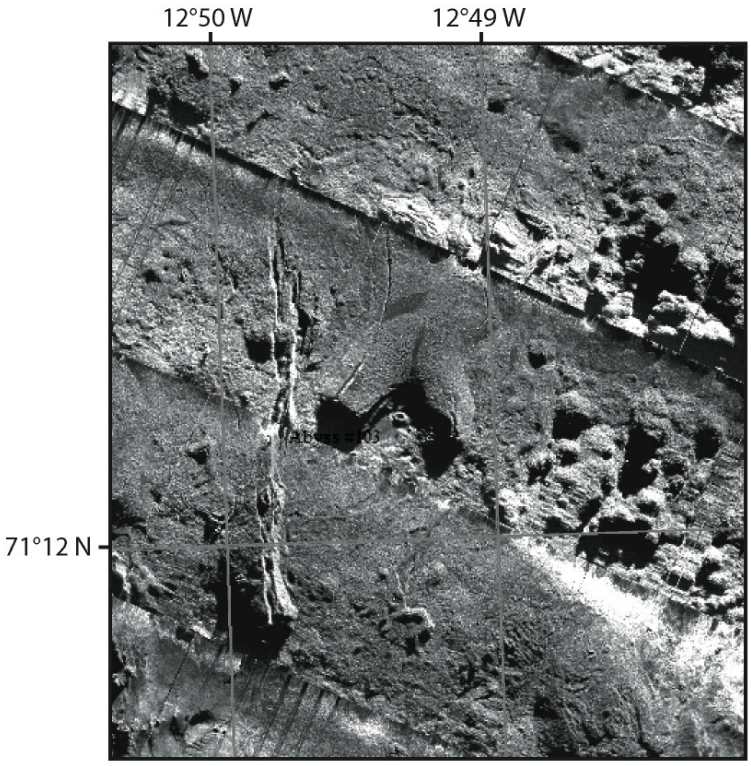

Figure 6.5: Sidescan sonar from Abyss #103 of a sheet flow on the axial valley floor. The large tumuli in the centre of the image may represent the location of the vent. Flow textures can be seen on the surface and hummocks on the right hand side.

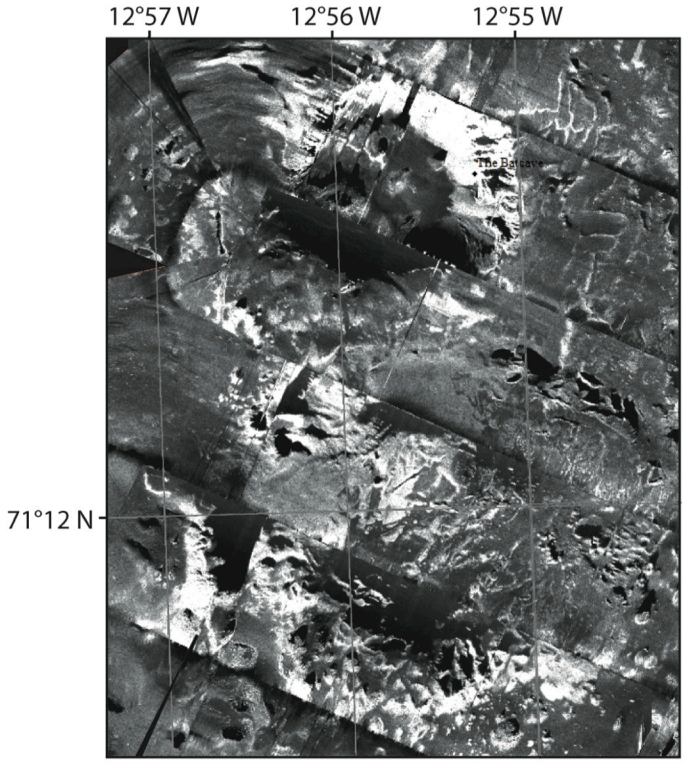

Figure 6.6: Sidescan sonar from Abyss #103 showing the two large features to the west of the inner valley. The upper is a large crater while the lower is a topographic high formed of blocky lavas, with a central crater. The lower one appears to have fed sheet flows out of its eastern side. Both are surrounded by relatively poorly backscattering sheet flows.

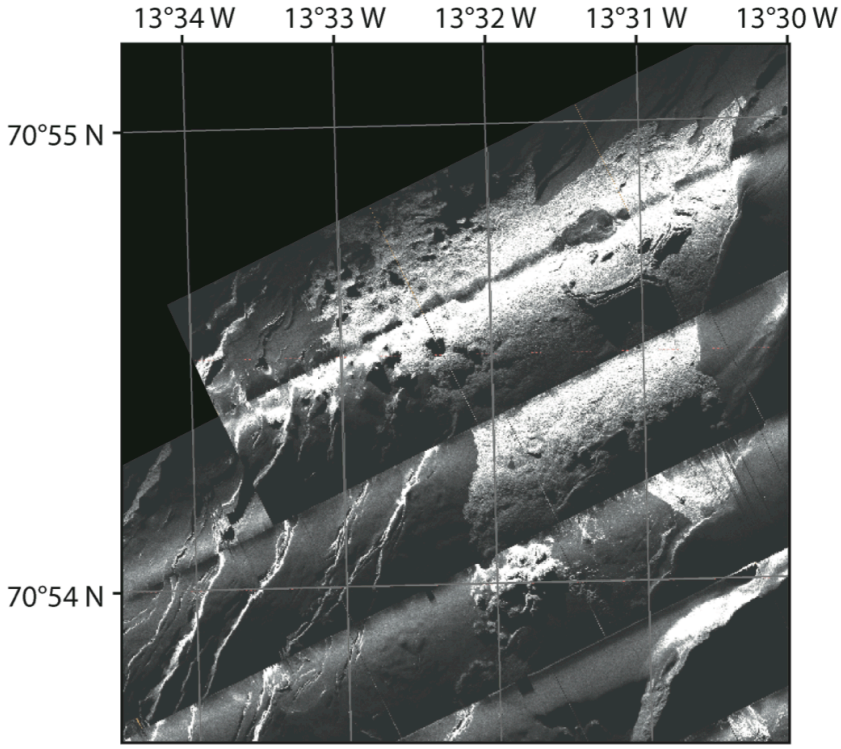

Figure 6.7: Sidescan sonar imagery from dive Abyss #104. Bright areas represent high levels of backscatter. This map shows a lava flow within the western half of the oblique valley flowing out over older sedimented seafloor. To the north the flow has flowed between faults, while to the east it appears to grade into increasingly hummocky terrain. Large tumuli can be clearly seen on the flow surface. Faulting to the west defines the westerly extent of the oblique valley.

6.3.7 Abyss #105 (Sidescan Sonar, 29.6 km^2)

Survey objectives: As survey #104 revealed volcanism on both sides of the tectonised area within the oblique valley, a second survey was designed to cover both possible volcanically active zones further south to access where the youngest and most voluminous volcanism was occurring. Survey 0105 covers two rectangular areas on either side of the shallower faulted terrain that splits the two possible axial valleys, as well as a single strip across this tectonic area to connect the boxes.

Geological description: Due to a technical fault, sidescan sonar data was only collected over the eastern valley. The survey shows volcanic morphology across the whole area, which takes the form of both sheet and hummocky eruptions. The brightest and probably young material observed centers on the high relief ridge at 70°46.25 N 013°31.85 W, taking the form of 50 – 200 m diameter hummocks on the ridge, surrounded by a brightly backscattering sheet or lobate lava flow. East of the ridge a second darker flow, with a similar form (hummocks on top of sheet flow terrain) is observed, corresponding with a second high relief area in the Seabeam bathymetry. Further dark looking, older lava flows can be observed between and around these flows. The area appears relatively untectonised, although clusters of axis parallel fissures can be found at 70°46.77 N 13°27.87 W and at 70°45.85 N 13°28.60 W where hummocks can be seen sitting on top of them.

6.3.8 Abyss #106 (Sidescan Sonar, 8.4 km^2)

Survey objectives: Survey #106 was designed to cover the volcanic looking seafloor in the western valley that was not covered by survey #105 (due to the fault). Due to a reoccurrence

of the technical fault the survey was not completed, however, a single strip across the shallower tectonised area was acquired.

Geological description: The strip shows relatively young looking reflective magmatism up to what is probably the base of the faults on the eastern side at 70°47.65 N 13°35.97 W (poorly resolved in the sidescan imagery). On the eastern side only one large and a few smaller, laterally discontinuous, easterly-dipping faults are observed. The top of the tectonised area is poorly reflective and heavily sedimented. All the faults east of 70°48.13 N 13°35.97 W dip to the east, but this changes west of this point and > 8 westerly dipping fault scarps can be observed. These faults are more closely spaced and brighter, suggesting that this tectonism may be more recent than that in the eastern valley. No volcanism is observed at the base of these faults, although as this is where the mission was terminated the imagery is not as clear as on the eastern side, and very little of the valley floor is covered.

6.3.9 Abyss #107 (Sidescan Sonar, 43.0 km^2)

Survey objectives: Survey #107 covers the floor of the axial valley between (and up to) the sidescan surveys collected in Abyss_#0102 and Abyss_#0103. This area covers the transition from the predominantly flat-topped seamount covered terrain and the flatter volcanic terrain, as long as providing continuous high-resolution observation along 28 km of the rift valley.

Geological description: The survey matches up well with the sidescan surveys that cross its northern and southern ends. The seafloor in the northern section of the survey area (71°20.73 N) is mostly hummocky (50–200 m in diameter) and not very brightly backscattering, suggesting these hummocks are not very young. Just south of this hummocky zone (71°20.25 N) the survey crosses several ~80 m high, westward dipping fault scarps. This area appears very dark in the sidescan sonar imagery and is unlikely to have experienced volcanism recently, a hypothesis supported by an area of very poorly backscattering dark hummocks just south of the faults. South of ~71°19.86 N brightness increases and an area of mixed sheet and hummocky lava flows are observed, with sheet flows becoming increasingly common further south. One small westward dipping fault appears to cut a section of this hummocky terrain around 71°15.19 N. Beyond this, purely sheet flows are observed extending for at least 3 km south to meet survey Abyss #0103 and covering an area in excess of 6.2 km^2. This area is fairly brightly backscattering and has a large (800 m long) tumulus roughly in the middle of the imaged area of the flow, which may be the source.

7 MAPR deployments (Laurila)

7.1 General information about the MAPR studies

Miniature Autonomous Plume Recorders [MAPR, see *Baker and Millburn*, 1997] are used for searching for evidence of hydrothermal activity in the water column. During POS-436, MAPRs were attached to the wire during rock (wax) coring and dredging. As the first station of the cruise, 3 MAPRs were attached to a dredge wire to measure the temperature of the sea water in this part of the Atlantic ocean and all 3 MAPR recorded a notable and reproducible double Nephel anomaly, accompanied by a temperature anomaly. One of the MAPRs (with what, during the course of the cruise, turned out to be the most stable Eh

sensor) also recorder a small Eh anomaly at a similar depth. A total of 33 deployments were done (details in Table 7.1). We had 5 MAPRs available. All of them were used at different times; however it was found that two of the MAPRs did not perform as well as the others.

7.2 Technical information about MAPRs

The MAPRs are instruments that record temperature, pressure, light-backscatter and Eh. Data from the light-backscatter sensor (LBSS or nephelometer) is recorded as a voltage. Conversion to nephelometric turbidity units (NTUs) could be done with equation 1. Raw data are used in this report (roughly 0,02V ≈ light attenuation of 0,01 m^{-1}).

$$\Delta NTU = (V_r - V_b)/a_n$$

Equation 1. ΔNTU= LBSS anomaly in excess of ambient seawater
V_r = raw voltage reading from the sensor
V_b =background voltage of the ambient seawater (i.e. , V_r before the plume interference)
a_n= a factor unique to each LBSS, which is determined with laboratory calibration.

Absolute temperature also was recorded. Temperature measurements could not be converted to temperature anomalies (Δθ), without information about the density profile.

Generally light attenuation anomalies define hydrothermal plumes better than their temperature (or Δθ) anomalies, because local hydrography and low salinity vent fluids restrict the Δθ signal. Nephel anomalies provide vectors towards a high temperature vent site because nephels are rarely from diffuse sources. Background Nephel concentrations varied greatly between MAPR units, and also as a result of differing turbidities in different water masses (see results).

The Eh sensor measures the seawater voltage with a Pt electrode. The absolute value of Eh varies significantly and drifts constantly during measuring. To eliminate this effect, the time derivative of Eh (Δ Eh) instead of absolute Eh were used in depth vs. Eh profiles. The random scatter in Δ Eh values varied between the different MAPR units. Also abundant scatter or varying rates of drift (seen as a change in the values between the way down and way up profiles) was recorded at multiple stations; these interferences did not prevent reliable interpretation at any station though. The Eh data was interpreted to show no anomalies if the profile was similar to some of the examples in **Error! Reference source not found.**; for details see results. The response of the Eh sensor should be roughly proportional to the age of the plume, as the reduced species in the plume are quickly oxidized by mixing and dilution with ambient seawater. Therefore, an Eh anomaly is usually only found close to the source. The data have not been converted to an absolute voltage against a standard hydrogen electrode.

Depth measurement is a function of pressure (db) and latitude; 71 was used for latitude at all locations, and depth calculated according to Fofonoff and Millard (1983).

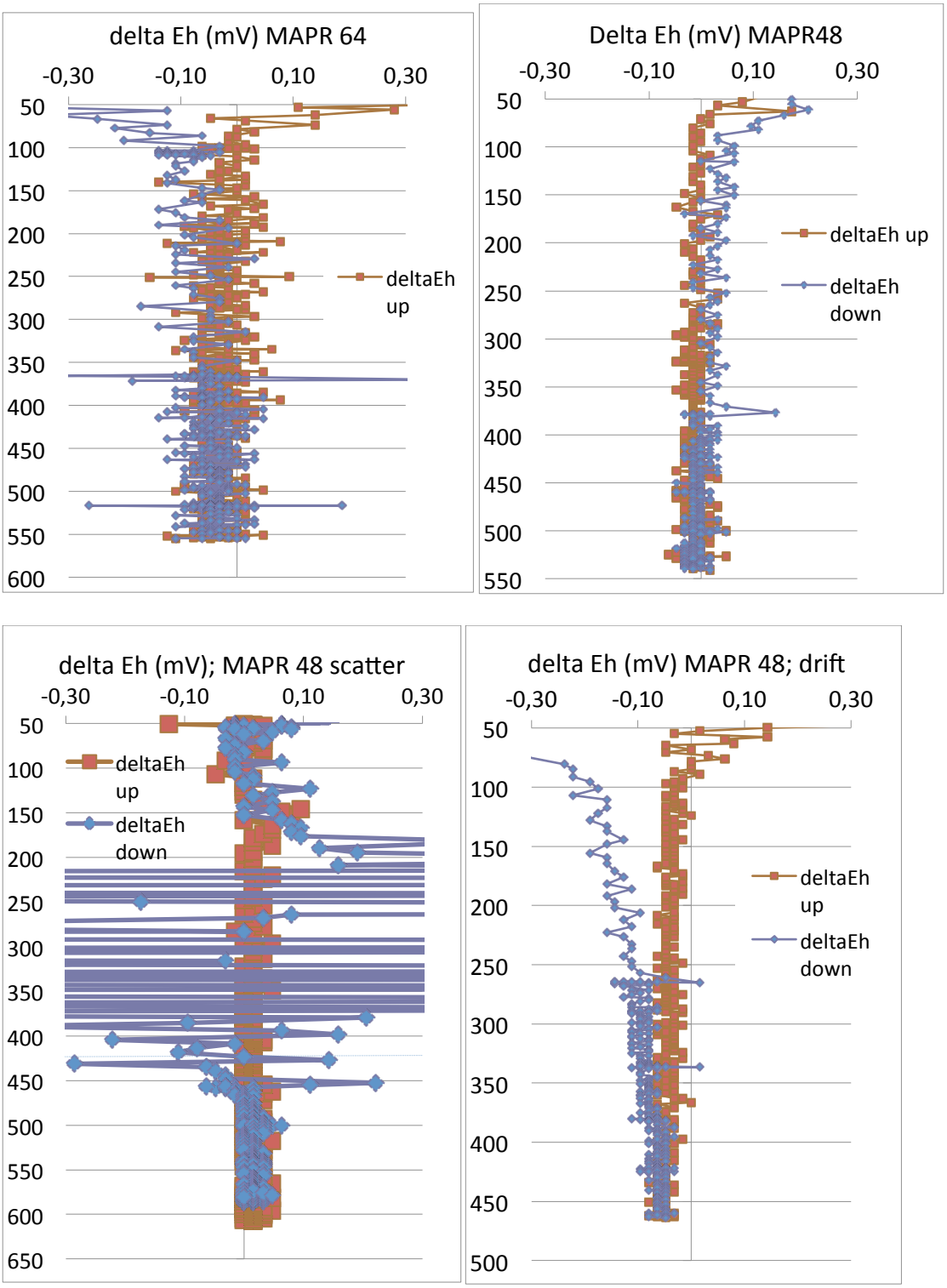

Figure 7.1: No anomaly was inferred from these Δ Eh profiles. On X-axis is Δ Eh in mV and on Y-axis is depth in meters.

7.3 Methods

A single MAPR was attached to the cable ~20 m above the rock corer. During these deployments, the MAPR was expected to reach a depth of ~15 m above sea floor. A MAPR was attached 200-350 m above the dredge bag to prevent any damage. During dredging the MAPRs reached variable depths. As a result we might have missed small-scale near bottom chronic hydrothermal venting at stations where the MAPRs were too high, although most

came within 100m of the seafloor. Deepest measurement from the MAPR are listed in Table 7.1. The depth of sea floor in the beginning and end of dredge targets are shown in Section 0 about sampling in this cruise report. Reasonably stable, chronic plumes are expected to appear no more than a couple of hundred meters above the seabed. Event plumes are found higher in the water column.

The longer bottom time for dredge deployments blurs the nephel vs. depth profile on the bottom leading to more(scattered) high values. Also the dredge might have mixed the bottom leading to higher nephel amounts.

MAPR showed some operational problems (e.g. very high scatter Eh plots), which later were interpret to perhaps reflect real changes in water properties. To monitor these changes at many sampling sites 2 MAPRs were attached to the wire in some cases.

At two locations we performed “MAPR” operations. At these stations, the dredge was used as weight at the end of wire but we did not intend to gain samples, instead 2 or 3 MAPR units were attached to the wire to prospect the water column for possible indications of hydrothermal activity.

A measurement interval of 5 seconds was used for all the measurements

7.4 Results

The very first station (MA-193) of the cruise was conducted in the northern part of the study area ~10 km east of the inferred spreading axis. The site is a depression reaching about 1 km deeper (=~3500 m) than the spreading axis to the West. 3 MAPRs were lowered to the seafloor; the configuration of measurements is shown in Figure 7.2. The depth reached by each MAPR (and their position to each other) can also be seen in Figure 7.3. All 3 MAPR units recorded a prominent double nephel anomaly at depth of ~1700-2300 m.

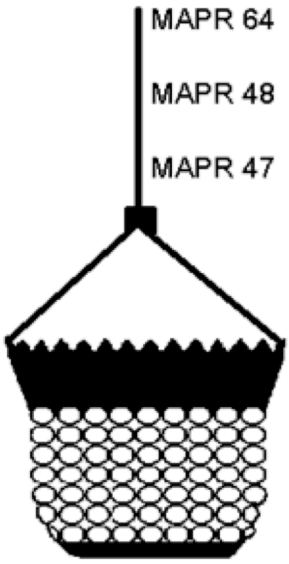

Figure 7.2: Configuration of MAPR studies at station MA_193.

According to nephels the detected anomaly was a “double plume”. The shallower and smaller anomaly was situated at ~1700-1900 m; at ~1900 m the Nephels returned shortly to background levels and immediately started to increase indicating the presence of a deeper (and larger) nephel anomaly. At around 2300 m the nephels once more returned to background levels, although this remained a bit higher at depth than at shallow water (a typical characteristic of water profiles recorded during POS_436). Depth vs. nephel profiles from each MAPR are shown in Figure 7.3 and are very consistent, showing the same behaviour on the way down and up in all 3 MAPR units. In Figure 7.3 we can also see that the back-ground level of nephels varies largely between the different nephel sensors.

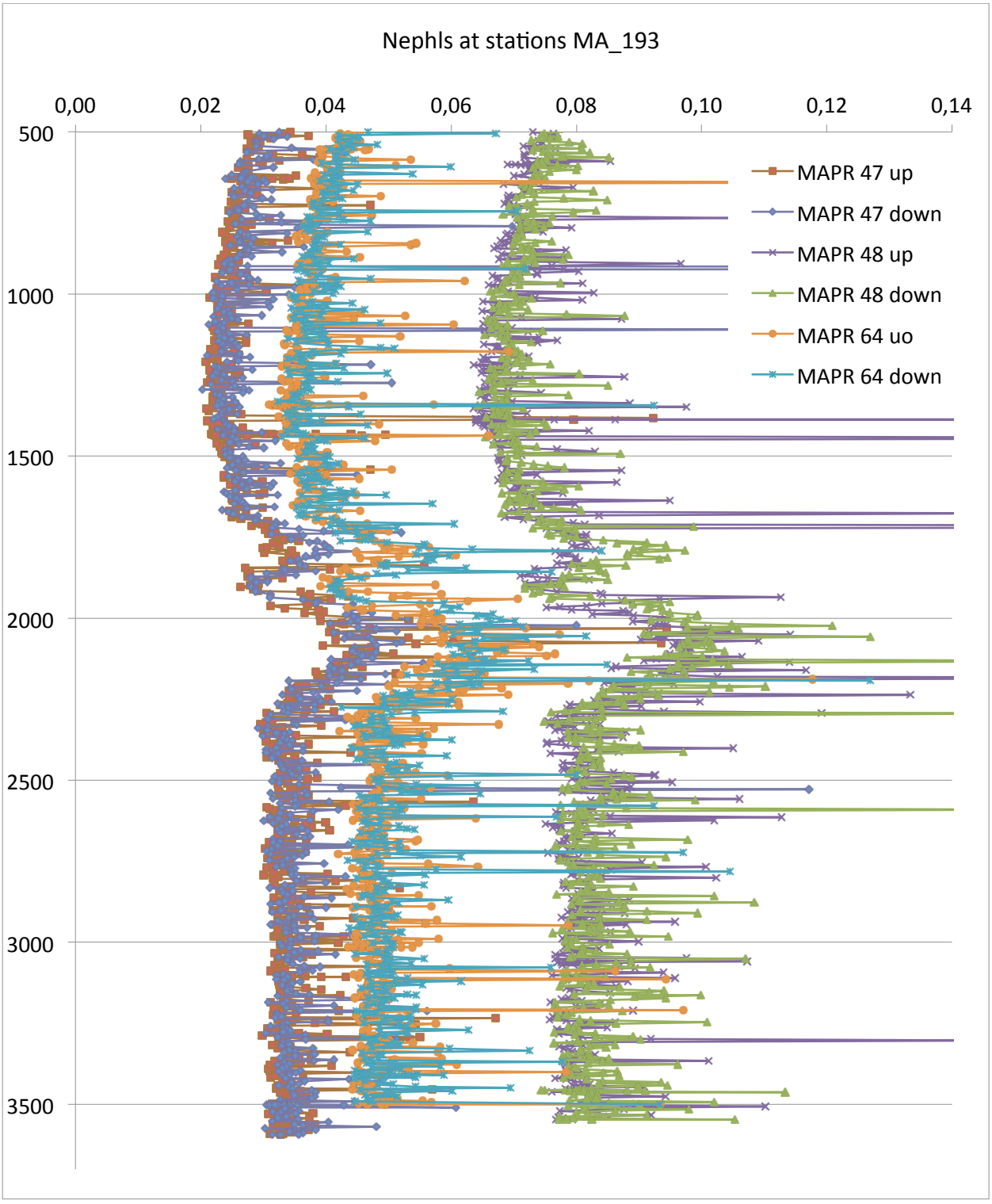

Figure 7.3: Amount of Nephels detected at station MA_193 where 3 MAPRs were attached to wire (at 50 m intervals, seen as different maximum depths) and lowered to the seafloor (Figure 2). Repeatable double plume anomalies were recorded in the depth interval 1700-2300. Different MAPR units have different background Nephel recording, but variance does not influence reliability of interpretation.

At station MA_193 the nephel anomaly was accompanied by a small Eh anomaly, which was recorded on the way up by MAPR 48 at the depth of 2100-2400 m (Figure 7.4). This potential Eh change in the water column was not recorded by MAPR 48 on the way down. Neither was it detected by any other MAPR unit. The lack of a repeatable signal might be due to water

currents, which possibly mix the water or/and due to masking by high scatter in measurements (typical to MAPRs 64 and 47).

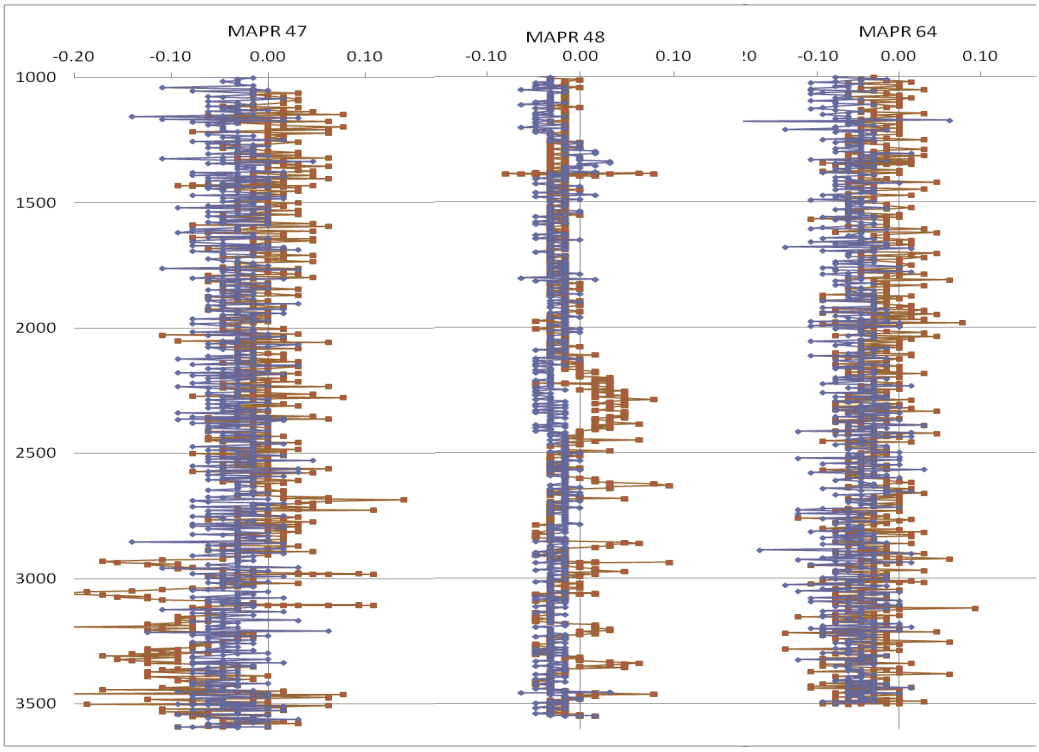

Figure 7.4: Eh measurements from different MAPRs at station MA_193, profiles are named after MAPR used; blue profiles mark the measurements on the way down and red profiles on the way up. MAPR 48, which is equipped with Eh sensor with least scatter, recorded a small Eh anomaly at depth 2100-2400 m depth, at the "bottom" of the deep plume inferred by nephel profiles.

On top of the prominent nephel and a possible Eh signal, slight temperature anomaly (0.01°C, which is normal value for hydrothermal influence on sea water at depth) was recorded at a depth of 1910-1960 m (Figure 7.5). This anomaly was recorded almost identically by all three MAPRs: at exactly same depth, shift to slightly colder on way down and to slightly warmer on the way up, furthermore the details of the positive anomaly were the same (small excursion to higher T at depth followed by larger and thicker excursion at shallower depth).

The whole temperature profile measured at station Ma_193 is also shown in Figure 7.5. As was typical for our stations during this cruise, temperature variations are seen at shallow water, then temperature drops below zero, reaching a minimum (<-0.8), after which temperature starts to increase slightly.

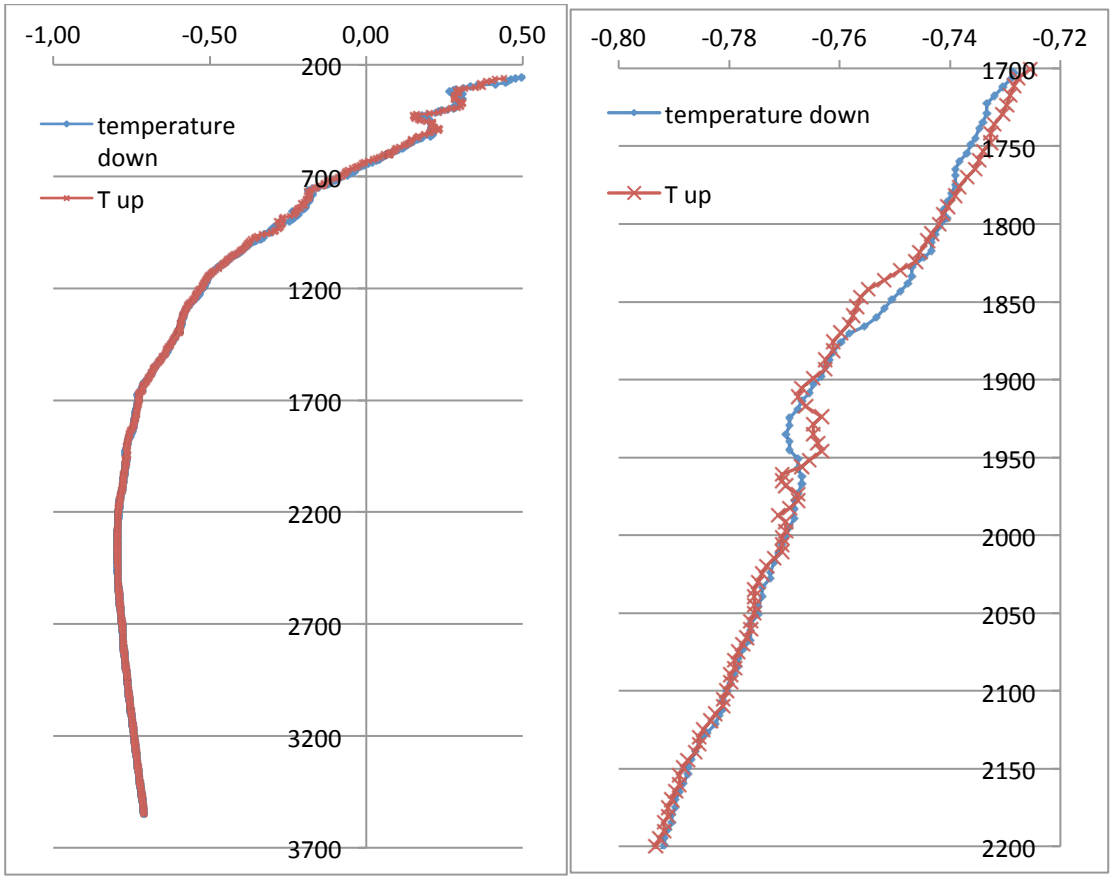

Figure 7.5: On the left diagram is plotted the whole temperature profile at station MA_193. Temperature changes are common in the shallow water. In the diagram on right is a detail of the temperature profile spanning the depth of plume signal inferred from other sensors (Eh and nephel). Here we have used data from MAPR 48, but temperature profiles were strikingly similar for each MAPR unit.

We interpret the plume anomaly measured at station MA_193 to have been created by hydrothermal activity at the adjacent ridge axis. The ridge axis is at about 2200 m depth, thus a plume from this ridge axis with a rise height of couple of hundred meters would fit to be the source of the detected anomaly. We do not know the hydrology of the area, but large increase in depth (>1 km for vertical distance of ~10 km) could encourage flow down along the flanks of the ridge axis. Thus it might be that after rise to the neutrally buoyant level the plume particles start to sink, creating the largest anomaly in the distal facies at bit deeper than the original rise height.

We did not detect any undisputable hydrothermal signal at any other stations during the cruise, with only one another “plume-like” Eh anomaly being recorded at station 226 (and at proper depth to possibly be caused by hydrothermal venting; Figure 7.6). It was small anomaly and not accompanied by changes in other measured sea water properties, so it was interpreted to indicate no presence of hydrothermal activity.

The general properties of the sea water column at Kolbeinsey seem to span a large variance. We had lots of “problems” with Eh sensors. These peculiarities were in the beginning thought to be operational problems with the Eh sensor in the MAPRs. In Figure 7.1 we presented some of the “end-member” Eh profile types. All of the examples in Figure 7.1 were interpreted to show no hydrothermal anomalies. We could not interpret the reason for large drift in the Eh profiles; often the Eh sensor only drifted on the way down or on the way up, sometimes Eh

profiles had sections with Eh drift and other parts were normal. All of the Eh sensors had their own “background scatter”, which varied according to the individual MAPR unit, which was interpreted to be normal variation. Instead, large amounts of “random scatter”, an example of which is shown in Figure 7.1 (lower left) for MAPR 48 at depth interval 200-400 m on the way down, was also often seen in the profiles. The reason for this “random scatter” during the whole deployment or during some parts of the deployment stays unresolved, but was not interpret to be due to hydrothermal activity. The amount of “random scatter” did not seem to vary between different MAPR units, all of the units showed it during some stations, and all of them showed coherent profiles at other stations. The “random scatter” was often (but not always) recorded by all of the MAPR units if deployment was done with multiple MAPRs on the wire. The largest correlation between the presence or absence of random scatter, seemed to be time; some days all the measurement had lots of random scatter, some days had none of it during all stations. When Eh profiles had lots of random scatter, usually the Nephel profiles had shifts to larger background values at depth (but this was not taken as an indication of hydrothermal activity as this change did not decrease before the sea floor). An example is given in Figure 7.7, in which we present data from MAPR 48 during example stations 244 and 249. Station 244 was done on 25th of July and shows high amounts of Eh scatter and deep Nephel high; similar profiles were recorded by MAPR 246, the only other stations with MAPR usage on 25th of July. On the next day stations 249 and 253 both had two MAPR on the wire to try to get at least one Eh profile without abundant scatter. All of the measurements done on 26th of July (MAPR 48 and 50 at station 249 and MAPR 48 and 50 at station 253) were excellent and low in random scatter; no deep Nephel highs were recorded. 25th of July was a stormy day, instead 26th was very calm and sunshiny. Maybe mixing of the bottom and shallow seawater causes the observed variation.

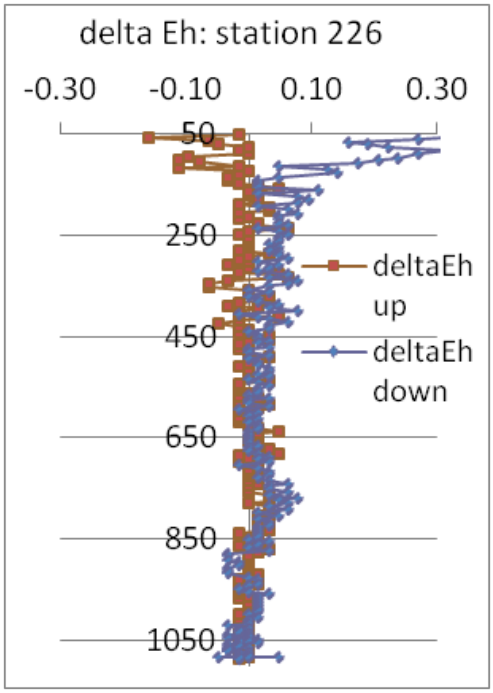

Figure 7.6: At station 226, a small Eh anomaly at “correct depth” was detected, but un-accompanied by changes in other measured sea water properties. Thus it was interpreted to not indicate presence of high-T hydrothermal venting.

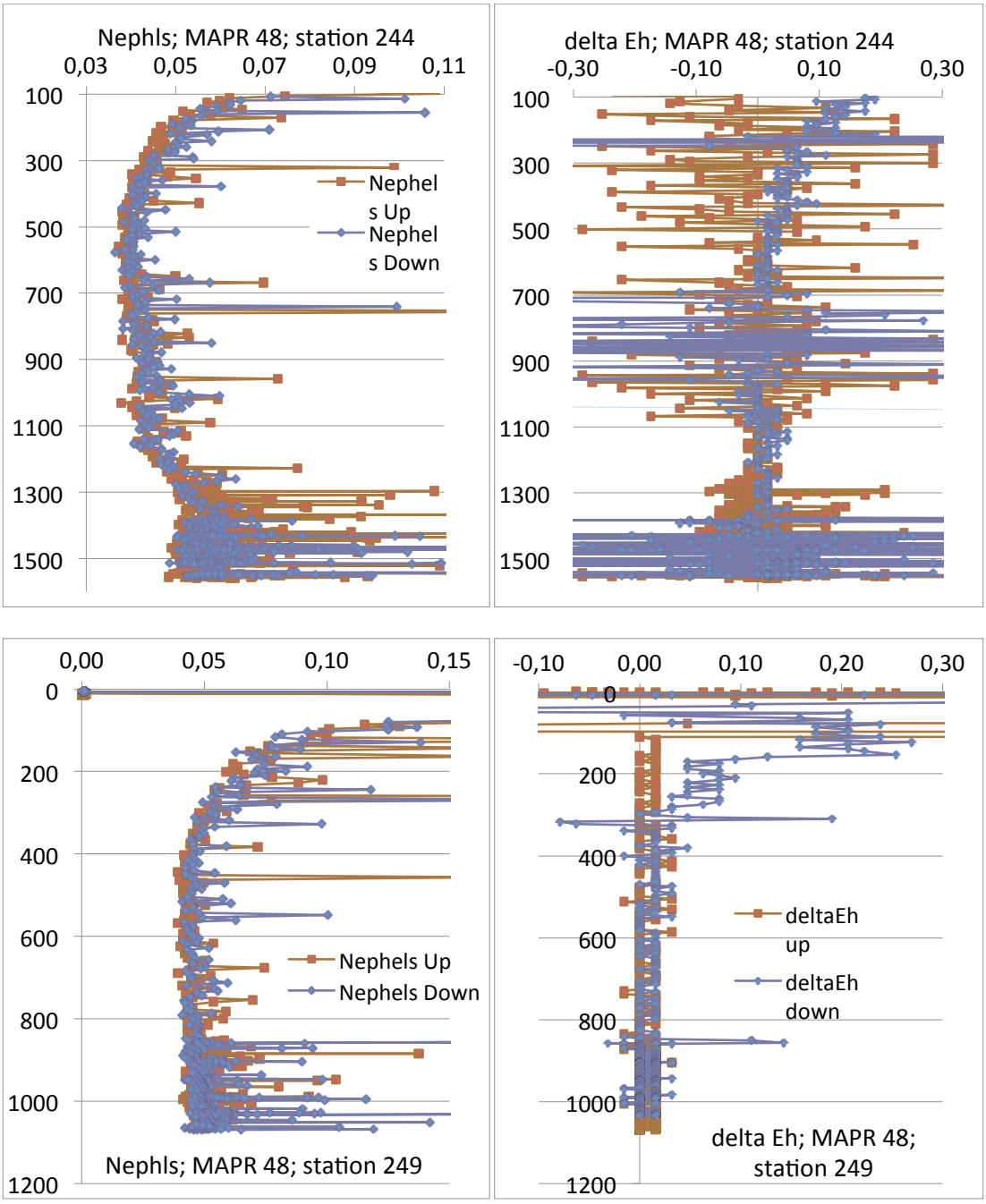

Figure 7.7: On the left: MAPR 48 at dredge station 244 on 25th July, compared to the same MAPR at station 249 the next day. At station 244 we see lots of "random scatter" in Eh, and shift to high Nephel background values at 1150 m depth; this is not an indication of hydrothermal activity as the change is very small and depth range of high values is large. Similar shifts to high background Nephel were seen at multiple stations. Same MAPR was used, so operational variance should be minimized. 25th of July was stormy day, as opposed to calm and sunny 26th; maybe scatter is caused by mixing of bottom and shallow sea water. The other stations done on these days 25th and 26th of July show same results. On 26th 2 MAPRs were used in the wire at both stations on that day and no scatter was recorded.

At one shallow station (DR_202), a temperature change (at about 120 m) was accompanied by a nephel anomaly (Figure 7.8). It might have been caused by hydrothermal activity, but a rise height of >350 meters would be required to create an anomaly at this level. A plume with that large rise height would probably cause much larger increases in T and Nephels, so this anomaly was interpreted to be due to plankton or other non-hydrothermal particle rich layer at shallow water.

The span in temperature profiles measured during cruise POS_436 is large, but most of the times if two MAPRs were used during one operation both MAPRs measured almost exactly the same profiles, thus the variation is real, not an artefact caused by large T change between lab and sea water. Commonly we omitted the large T shifts typical to shallow water (in the upper 100-400 m). Studying T changes at shallow water in more detail reveals that sometimes a small temperature increase measured on the way down was changed to similar decrease on the up, or the other way around (keep in mind that also location might have changed due to movement of the ship during dredging). Small scale changes were common, but also 100 meter scale variation was observed between different days and locations. In figure 9 we present some of the T profiles, many others were recorded as well. Generally these changes were interpreted as mixing of shallow water and not indication of hydrothermal activity.

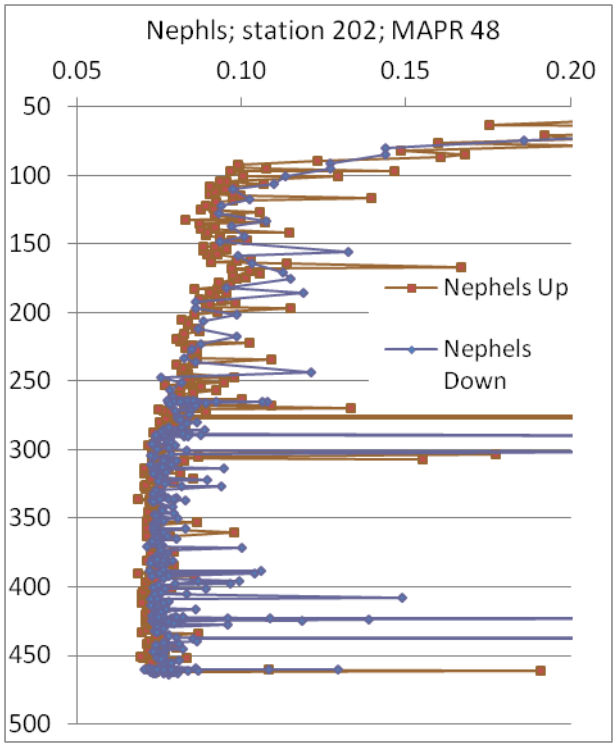

Figure 7.8: A small anomaly detected at station 202 was the only other Nephel anomaly (than at station 193) detected during POS_436. It was perhaps accompanied by temperature anomaly (or T anomaly was normal changes in temperature at shallow water; see Fig.9). Rise height of >400 m would be needed to create this anomaly via hydrothermal processes, thus the anomaly was not interpreted to be created by hydrothermal activity.

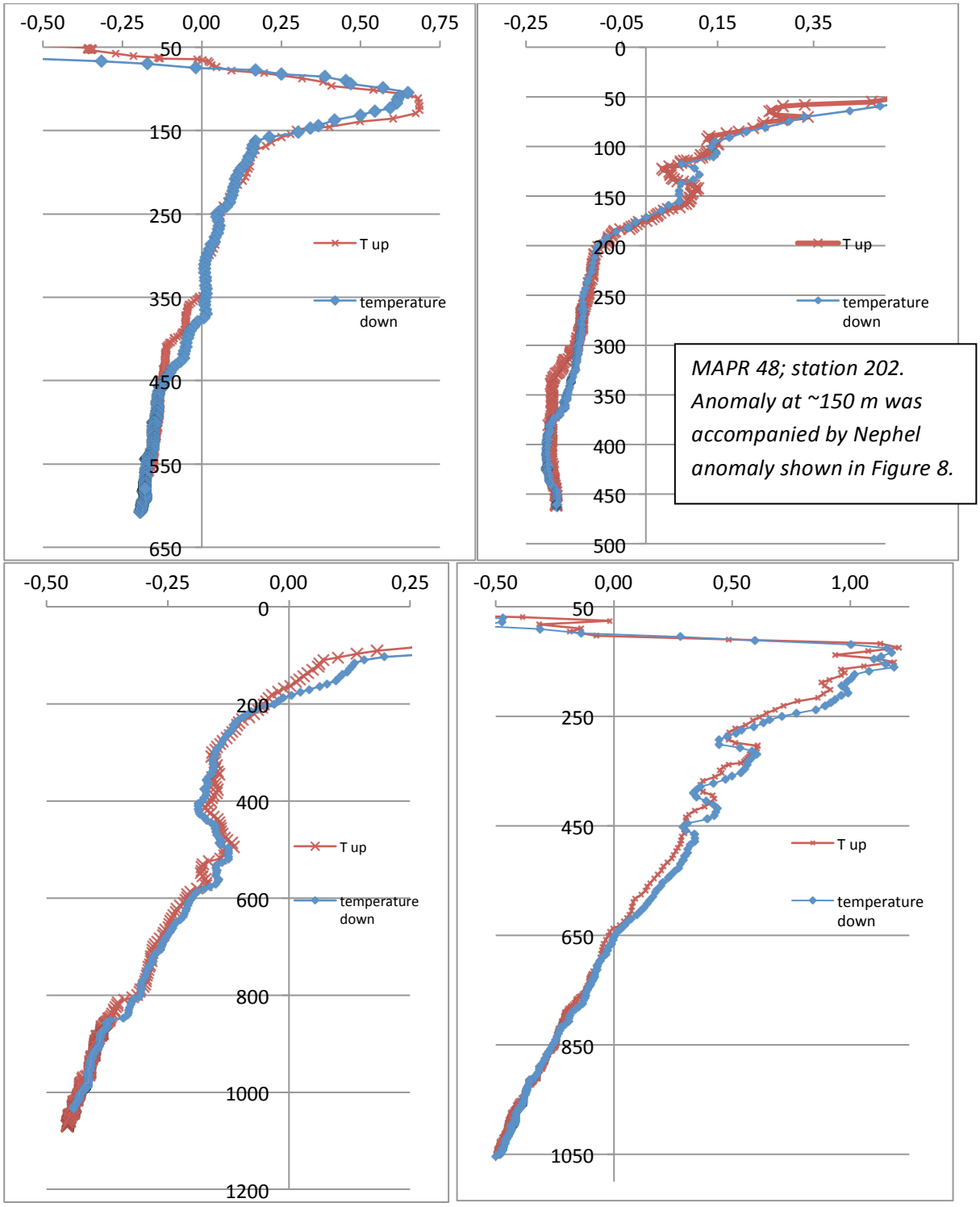

Figure 7.9: Examples of different T profiles recorded during POS_436. Lots of variation in the water stratification were observed at shallow water, but also large changes (increased or decreases) at deeper levels were common. Most often the deepest 100-200 m had stable temperature. The absolute temperature of this water though varied a lot; according to depth, but also temperature at same depth varied from station to station. Notice different horizontal and vertical scales.

Table 7.1: Details of the MAPR usage during POS-436.

Date	File name	station ID	MAPR No	Start time	at depth	end time	max depth	Details of the deployment
13/07/2012	dr 1	MA 193	47	5.00	6.18	7.39	3593	plume
13/07/2012	dr 2	MA 193	48	5.00	6.18	7.34	3547	plume
13/07/2012	dr 3	MA 193	64	5.00	6.18	7.37	3500	plume
15/07/2012	DR 196	DR 197	48	11.25	12.23	13	456	Hit bottom
16/07/2012	DR 200	DR 200	47	6.16	7.08	7.35	423	Eh strange
16/07/2012	DR 201	DR 201	64	8.39	9.15	9.4	402	Eh drift
16/07/2012	DR 202	DR 202	48	10.35	11.20	11.46	463	Small Nephel @ 170 m
16/07/2012	DR 202	DR 202	64	10.35	11.20	11.5	547	Small Nephel @ 170 m
16/07/2012	DR 203	DR 203	50	12.58	13.26	14.02	498	Eh drift
16/07/2012	DR 203	DR 203	64	12.57	13.26	14	460	Small Nephel @ 220 m
18/07/2012	DR 207	DR 208	50	6.15	7.13	7.51	1355	Lots Eh scatter
18/07/2012	DR 208	DR 209	48	9.05	9.37	10	1035	Scatter in Eh
18/07/2012	DR 208	DR 209	64	9.05	9.37	9.56	996	Scatter in Eh
18/07/2012	DR 210	DR 210	48	10.35	11.14	11.4	1082	All Ok, no anomaly
18/07/2012	DR 210	DR 210	64	10.35	11.14	11.43	1134	nephel drift
18/07/2012	DR 211	DR 211	47	12.11	12.50	13.2	1010	Eh scatter
18/07/2012	DR 211	DR 211	48	12.09	12.48	13.22	1064	All OK, no anomaly
19/07/2012	DR 214	DR 214	48	6.10	7.03	7.46	1793	Small nephel @ 1500
19/07/2012	DR 215	DR 215	48	8.27	9.27	10.02	1610	High deep nephels
19/07/2012	DR 216	DR 216	48	11.15	12.28	13.18	2173	High deep nephels
19/07/2012	DR 217	DR 217	48	13.44	14.50	15.47	1897	Hit sea floor ?
20/07/2012	DR 226	DR 226	48	12.58	13.35	13.52	1085	Small Eh & neph @790
22/07/2012	DR 231	DR 231	48	7.54	8.37	9.04	540	Some Eh scatter
22/07/2012	DR 232	DR 232	48	10.00	10.39	11.17	524	All OK, no anomaly
22/07/2012	DR 233	DR 233	48	12.00	12.40	13.09	608	Eh scatter
22/07/2012	DR 233	DR 233	50	12.02	12.40	13.06	558	Eh drift

22/07/2012	DR 234	DR 234	48	13.49	14.29	15.03	400	Eh drift
22/07/2012	DR 235	DR 235	49	16.15	16.53	17.2	358	Eh scatter
23/07/2012	DR 237	DR 237	48	8.01	8.48	9.23	1194	High deep nephels
23/07/2012	DR 238	DR 238	48	10.11	10.54	11.29	1250	High deep nephels
23/07/2012	DR 240	DR 240	48	16.10	16.57	17.34	1078	Eh drift at shallow
24/07/2012	DR 242	DR 242	48	9.27	10.20	11.01	1437	High deep nephels, Eh scatter
25/07/2012	DR 244	DR 246	48	10.09	10.55	11.4	1548	High deep nephels, Eh scatter
25/07/2012	DR 245	DR 247	48	12.50	14.55	15.43	1996	High deep nephels, Eh scatter
25/07/2012	DR 246	DR 248	49	16.34	17.33	18.16	1528	High deep nephels, Eh scatter
26/07/2012	DR 249	DR 250	48	7.53	8.45	9.13	1069	All Ok, no anomalies
26/07/2012	DR 249	DR 250	50	8.00	8.45	9.14	1099	All Ok, no anomalies
26/07/2012	DR 250	DR 252	50	9.4	12.18	13.25	1290	Eh scatter on way down
26/07/2012	M 253	MA 253	48	16.45	16.51	16.54	218	Crater, very shallow
26/07/2012	M 253	MA 253	50	16.45	16.51	16.54	166	Crater, very shallow
27/07/2012	DR 256	DR 256	48	13.47	14.26	14.56	619	All OK
27/07/2012	DR 257	DR 257	48	16.04	17.01	17.27	557	Eh scatter @ 350
28/07/2012	DR 261	DR 261	48	10.41	11.47	12.44	1577	Hit the seafloor

8 Volcanic activity of the Northern Kolbeinsey Ridge - a summary of sampling results (Elkins)

A major goal of the expedition was to accurately position previous sampling attempts and deliberately target active volcanism with new sampling efforts. Sampling targets (both dredge and wax core) were selected to retrieve fresh basalt material from mapped areas of interest (Figure 9.1). In some areas the most obvious choices for targeted sampling (e.g. flat-topped volcanic cones) produced overall relatively weathered, altered basalt samples with variable sedimentation. In other areas, relatively fresh material was retrieved by dredge or wax corer; the chances of such success were greatly enhanced by high-resolution AUV maps.

In the most northerly section of the mapped area, few dredges returned fresh basaltic material, suggesting that it is only sporadically volcanically active. As the ship multibeam mapping was generally of lower quality in deeper waters, such that small features (like hummocky shapes or possibly sheet flow targets) could not be identified it is possible that sampling was somewhat biased: nonetheless, all of the volcanic features sampled were relatively old and altered.

South of the most northerly area, the style of volcanism changes from dominantly individual, flat-topped volcanic centers to more hummocky terrains and sheet flows. The flat-topped volcanoes that do exist in this region also appear younger and less altered than to the north. A number of fresh basalt targets were sampled in this region, suggesting that the progressively shallower terrain has higher magma flux.

The shallow, central portion of the map area is located along the Eggvin Bank bathymetric high. The style of volcanism continues to be dominated by sheet flows and hummocky terrains in the valley floors. The Eggvin Bank area contains two parallel axial valleys. Our sampling and mapping suggested that the eastern valley contains fresher material than in the west, suggesting an axial relocation toward the east has happened relatively recently. The major eastern bounding fault of the eastern axial valley is straddled by a large single volcanic cone (Mt. Eggvin), which may be the cause of the axial relocation—i.e. the high magma supply to Mt. Eggvin may have effectively pulled the axis eastward. The flanks of the volcano are covered in basaltic flows of varying age, as evidenced by different degrees of sample freshness. The volcanic crater, which is overall no deeper than 200 m, contains extremely young, fresh, vesicular, popping basalt rocks.

The southernmost portion of the map area terminates in an overlapping spreading center east of the northern tip of the middle Kolbeinsey Ridge segment. An apparent transfer fault west of the neovolcanic zone in the central map area connects to a more westerly valley. Again, an overlapping, parallel second axial valley is located on the eastern side of the segment; in this case, however, both the western and eastern valleys contained both relatively fresh, and more altered and sedimented volcanic material. Overall the freshest volcanic rocks were dredged and cored from sheet or hummocky flows, rather than the flat-topped volcanic cones, which overall appear to be older. No apparent fresh volcanic targets were identified by our mapping efforts further toward the southern edge of the spreading center in either valley. However, as in the north, the multibeam results in the far south are less well resolved due to increasing depth and poor weather during mapping. It is thus at present unclear which of the two overlapping axial valleys in the south is more volcanically active and which is likely waning.

9 Sampling (dredge, wax corer) and MAPR station list with sample descriptions (v.d. Zwan, Elkins, Laurila, Meisenhelder, Rivers)

Total: 35 dredges, from which 26 dredges had rock recovery. 6 wax corer samples. 2 AUV samples. All samples are stored in Kiel (12 rock boxes, 1 box with glass and dropstones), unless otherwise noted.

Station abbreviations: DR = Chainbag dredge (Kettensack Dredge); VSR = Wax corer (Vulkanitstoßrohr); AUV = Sample taken by AUV by colliding.

Station Area	Latitude (°N)/ Longitude (°W)	Date/ Time (UTC)	Depth (m)	MAPR nr.	Sample descriptions and samples taken (Gl = Glass; Pl = Plagioclase; Ol = Olivine; BMC = rock/glass to Bryn Mawr College, USA; Kiel = rock/glass to Geomar, Germany)
193 MAPR	71°08.088'/13°03.395'	13.07.12 5:13 – 7:29	3800	47 at 10 m 48 at 60 m 64 at 110 m	No dredging.
197 DR North side of Eggvin shoals axial high (central NKR); N(E) volcano of volcano ridge in center axis	71°08.088'/13°03.395' to 71°08.229'/13°02.811'	15.07.12 11:52 - 13:04	482 - 448	48 at 200 m Bottom hit	Half full with mud and ~50 cm-dm pieces of old basalt and rounded dropstones **1**: 6x5x2 cm: Angular basalt piece, top covered with glass crust (2 mm thick). Gray and reddish alteration. 5% Vesicles (<2 mm) + few larger vesicles (~1 cm). **2**: a) 8x6x5 cm b) 4.5x3x3 cm. Blocky basalt, some red crust, moderate alteration. Top glassy crust (2 mm thick). Gray to brown. 10% vesicles (<1 mm – 1 cm). b) slightly more altered **3**: 8x7x4 cm: Sub angular basalt. Red coating on surface/in vesicles. 40% vesicles (2 mm – 1 cm). Dark grey to dark brown. **4**: 7.5x5x4 cm: Sub rounded basalt. Altered red surfaces, not glassy. 10% vesicles (< 4 mm). Dark gray/ red alteration. **5**: Angular to sub-angular basalt. Moderate alteration. 30% vesicles (1-5 mm). Dark grey to reddish brown. **6**: 6x4x3 cm: Rounded basalt. Red brown alteration. Flow structures? No glass. 5% vesicles (<1 mm – 8 mm). Extra rocks: 7 assorted dropstones, rounded, reddish. 6 basalts, mostly angular, moderately altered and vesicular. Little glass.
200 DR Ridge N of Eggvin (central NKR), N volcano of active ridge	71°04.271'/13°08.214' to 71°04.475'/13°07.527'	16.07.12 6:30 - 7:40	527 - 570	47 at 300 m	1 Big rock + ¼ dredge full of (glassy) basalts semifresh-altered, dropstones, sponges. **1**: 16x12x11 cm: Glassy basalt block, brown to gray interior. Moderately altered. 5% vesicles (<2 mm). Two glassy surfaces up to 5 mm thick. Glass has some red surface alteration, rest is black fresh. **2xGl** (Kiel, BMC) **1** to BMC. **2**: 17x9x8 cm: Portion of thick basalt flow. 2-3 mm black glass on top, covered by reddish altered flow top. Gray to red-brown interior, moderately altered. 10% vesicles (1 mm). **3**: 15x13x8 cm: Pillow fragment with brown basalt interior (altered). 10-20% vesicles (2-4 mm) ~2 mm glassy rind, black with some red alteration. **4**: 11x9x6 cm: Oblong pillow. Red-brown, altered interior, <1 cm glassy rind, black with red alteration. Vesicles throughout (10-15%, 2 mm). **5**: a) 8x7x4 cm b) 8x5x3 cm c) 8x5x3 cm: Thin basalt sheets with glass on two sides. Gray to red brown, moderately altered. 20-30% vesicles (2 mm – 1 cm). Glass rind 3 mm – 1 cm thick, mostly fresh. Colourless phenocrysts (Pl?) up to 8 mm (< 5%). **2xGl** (Kiel, BMC) **6**: 12x9x7 cm: Basalt block, grey to brown with moderate alteration, 20-30% vesicles (1-4 mm). Extra rocks: 7 assorted dropstones, 3 cm -16 cm. 8 basalt samples, variably altered, vesicular and glassy, black to gray to red-brown

Station Area	Latitude (°N)/ Longitude (°W)	Date/ Time (UTC)	Depth (m)	MAPR nr.	Sample descriptions and samples taken (Gl = Glass; Pl = Plagioclase; Ol = Olivine; BMC = rock/glass to Bryn Mawr College, USA; Kiel = rock/glass to Geomar, Germany)
201 DR Ridge N of Eggvin. (central NKR) S bathymetric fresh, hummocky ridge	71°02.711'/13°09.541' to 71°02.910'/13°08.977'	16.07.12 08:36 - 09:45	526 - 516	64 at 300 m	Full, basalt rocks, some glassy. Vesicular. Some dropstones. **1**: ~50x40x40 cm (taken interior piece (32x13x11 cm) + glass): Basalt block. Subangular. 30% vesicular (1-7 mm). Glass encrustation on multiple sides (<1 cm thick). Moderately altered. Gray/darkbrown. Orange/yellow in altered parts. **2xGl** (Kiel, BMC). **2**: 30x22x20 cm: Subangular pillow (?) basalt (roundish). Moderately altered glass encrustations (mm's thick). 5-20% vesicularity (1-5 mm). Dark gray/brown. Some reddish on altered parts. **3**: 14x14x14 cm: Thick blocky sheetflow. Moderately altered. 10% vesicularity (1 mm, some up to 1 cm). Dark gray, some reddish brown. Some round (flow?) structures on surface. Glassy fragments on both sides (< 2 mm thick). **1xGl** (Kiel) **4**: a) 9x7x5 cm b)7x6x5 cm: Thin sheet flow with glass on both sides, sub angular. Pretty altered. Glass encrustations (3 mm thick). 5% Vesicular (1-3 mm). Reddish + dark grey. Sample b has round edge surface (pillow like?). Up to 3 mm large Pl (?) phenocrysts (~1%). Partially covered by yellow mud crust. **5**: 12x10x6 cm: Blocky basalt block. <5% vesicularity (3 mm). Reddish brown, some gray. **6**: 10x6x5 cm: Basalt block, subangular. No encrustations/glass. 50% vesicularity (3-6 mm). Dark brown. Extra rocks: 7 assorted dropstones. 5 basalt samples. Variably glassy, vesicular, altered.
202 DR Small volcano S of Hummocky ridge (central NKR)	71°01.585'/13°11.062' to 71°01.744'/13°10.414'	16.07.12 10:40 - 11:55	750 – 601	64 at 400 m 48 at 500 m	Full with mud, no rocks.
203 DR Small volcano S of Hummocky ridge (central NKR). S of 202DR.	71°00.313'/13°10.948' to 71°00.491'/13°10.320'	16.07.12 12:48 - 14:10	721 – 645	50 at 400 m 64 at 450 m	4 ½ basalt rocks + 5 dropstones. **1**: a) 10x7x5 cm (+ small piece) b) 3x2x1 cm: Porous basalt block (tephra?) with cm sized glass fragments. 30% vesicular (<2 mm). Reddish alteration (moderate). Glass semi-fresh. **2xGl** (BMC, only small grains to Kiel) **2**: 10x5x5 cm: Basalt sheet flow with glass on 2 sides (2 mm & 5 mm thick). 7% vesicularity (1 mm – 1 cm, irregularly distributed). **3**: 16x11x8 cm: Angular basalt block. Brownish-red alteration. Dense, no vesicles, no glass. **4**: 6x4½x4 cm: Basalt block. Brownish-red alteration on surface. Gray inside. Vesicles 5%, 10% on surfaces (1-4 mm). Pl crystal 5 mm, <1%). Extra rocks: 5 assorted dropstones.
208 DR Hummocky terrain (N NKR), N of volcanic cone with sharp ridges	71°22.587'/12°35.200' to 71°22.703'/12°34.576'	18.07.12 6:21 - 7:57	1472 – 1480	50 at 300 m	2 big (50 cm) + 6 small (dm's) fresh basalt rocks with glass (1 big back). **1**: 40x32x30 cm: Pillow basalt. Dark gray. Glass rind of 2-4 mm thick, mostly black, some palagonite on top. Vesicles <5% (1 mm). Zone with no vesicles, close to top, following the surface. Fresh (slightly less than 2). **2**: a) 12x9x5 cm b) 7x5x4 cm: Sheet flow/pillow rim. Dark gray, black (fresh). Vesicles <5 % (1-3 mm). 2 glass rims. Top 1 cm thick, bottom ~5 mm. On top palagonite. Flow/bubble rim structures on bottom. **2xGl** (Kiel, BMC). **2a + b** to BMC. Extra rocks: 1 extra basalt as **1** (nr. 1) 3 extra basalt as **2** (nr. 2-4)

Station Area	Latitude (°N)/ Longitude (°W)	Date/ Time (UTC)	Depth (m)	MAPR nr.	Sample descriptions and samples taken (Gl = Glass; Pl = Plagioclase; Ol = Olivine; BMC = rock/glass to Bryn Mawr College, USA; Kiel = rock/glass to Geomar, Germany)
209 DR Small volcano, S of volcanic cone with sharp ridges. N NKR	71°18.805'/12°42.163' to 71°18.955'/12°41.668'	18.07.12 9:18 - 10:04	1199 – 1205	48 at 300 m 64 at 350 m	~30 medium to small (5-20 cm) basalt sheet flows/pillow fragments. **1**: 17x13x8 cm: Basalt block/thick sheet/outer pillow rim? (rounded). Fresh glass rim on top (~4 mm thick) + bottom (~5 mm thick). Some palagonite, some 'greasy' start of glass alteration appearance. Black-grey basalt, <5% vesicular (irregular formed, 1-10 mm). 1% Ol phenocrysts up to 7 mm. <1% Pl phenocrysts up to 7 mm. **2**: a) 7x6x3 cm b) 7x5x4 cm: Sheet basalt. Top up to 1 cm thick glass rind. Minor palagonite, slightly greasy. Smooth, irregular, glass free bottom. Grey-brown basalt. Vesicularity ~5%, irregular distributed (1-5 mm). <1% Pl + Ol up to 7 mm. **2A**: **2xGl** (Kiel, BMC). **3**: 13x13x7 cm: Thick sheet flow/pillow rim. Basalt with 5 mm thick glass rind on top, covered by very thin palagonite, showing flow structures. Basalt fresh grey (to brown). 10% Vesicularity (1-10 mm). 1% Ol phenocrysts up to 7 mm. Bottom big holes (1-2 cm) texture with rims in between. **4**: 6x4x1 ½ cm: Basalt thin sheet flow. Thin mm glass rim. Smooth surfaces, slightly palagonite covered with flow/sink structures. Basalt fresh grey. Vesicularity 2% (1-3 mm). No visible crystals. Extra rocks: 5 extra basalts as 1 and 2 (nr. 1-5) 2 extra basalts as 4 (nr. 6-7)
210 DR Small flat-topped volcano west of volcanic cone with sharp ridges. N NKR	71°20.442'/12°41.269' to 71°20.518'/12°40.608'	18.07.12 10:37 - 11:50	1273 – 1115	64 at 300 m 48 at 350 m	2 glassy basalt rocks (10-20 cm) **1**: 16x12x11 cm: Pillow (end) basalt with 1-4 mm thick glass rim. Fresh glass (no-minor palagonite). Dark grey basalt, 2% vesicles (1-3 mm). No phenocrysts visible. **2xGl** (Kiel, BMC). **2**: 15x11x5 cm: Similar as 1. **2xGl** (Kiel, BMC).
211 DR Volcanic cone with sharp ridges. N NKR.	71°20.209'/12°38.164' to 71°20.420'/12°37.665'	18.07.12 12:09 - 13:29	1380 – 1250	48 at 400 m 47 at 450 m	Empty
214 DR Hummocky terrain Northern most NKR	71°27.223'/12°24.335' to 71°27.348'/12°23.731'	19.07.12 6:18 - 7:50	1880 – 1820	48 at 260 m	4 Rocks basalt, semi-fresh **1**: 10x9x8 cm: Basalt rock angular. Top glass rind of 1-2 mm thick (fresh black). Basalt altered, yellow-red-greybrown. Inside dark grey. Vesicularity <5% (1-7 mm). **2**: 16x10x8 cm (in 3 pieces): Basalt block angular. 2 mm thick glass patches on top, rest of the top smooth. Orange-grey-yellow-white altered. Vesicularity 5% (1-10 mm). Inside light gray. More altered as 1. Extra rocks: 2 extra basalts, similar, slightly more palagonite.
215 DR Small, clear, flat-topped volcano west of 214DR. N NKR	71°28.596'/12°23.630' to 71°28.558'/12°24.370'	19.07.12 8:32 - 10:10	1819 – 1703	48 at 300 m	10 Basaltic pillow fragment samples. **1**: 26x20x16 cm: Pillow basalt with black glass rind of 1-4 mm thick. Some areas with little palagonite. Grey basalt (with a partially brown-red layer). Vesicularity 10% in a 3 cm layer, 1 cm below the rind (1-3 mm). Otherwise <1% vesicles. **2xGl** (Kiel, BMC). **2**: 14x11x11 cm: Pillow basalt with black glass, similar as **1; 2xGl** (Kiel, BMC). **2** to BMC Extra rocks: 4 extra basalt samples, similar as **1**
216 DR Hummocky hill with crater, E of clear volcano N NKR	71°31.976'/12°14.270' to 71°31.972'/12°15.228'	19.07.12 11:23 - 13:15	2360 – 2209	48 at 300 m	Empty.

Station Area	Latitude (°N)/ Longitude (°W)	Date/ Time (UTC)	Depth (m)	MAPR nr.	Sample descriptions and samples taken (Gl = Glass; Pl = Plagioclase; Ol = Olivine; BMC = rock/glass to Bryn Mawr College, USA; Kiel = rock/glass to Geomar, Germany)
217 DR Clear flat-topped volcanic cone N NKR	71°32.162'/12°17.507' to 71°32.110'/12°18.575'	19.07.12 13:39 - 15:55	2087 – 1883	48 at 300 m	15 (10-30 cm) Glassy basalts (with much of life/mud on there) **1**: 25x24x18 cm: Blocky basalt, with rough (a-a structure) surface. Seem to consist of multiple fragments welded together (glass in between): breccias appearance. Grey brown basalt. Black glass, irregular in patches (of 1 mm – 1 cm thick). Moderately weathered (greasy luster). Or cracked basalt, rather than glass? Vesicularity <1% (1 mm). Pl phenocrysts in basalt 5% (1-3 mm). **2**: 20x12x12 cm: Basalt flow/rock. Top covered by glass with uneven thickness up to 2 cm. Palagonite on the glass. Vesicularity <1% (up to 2 mm). Pl phenocrysts 3% (up to 4 mm). **2xGl** (Kiel, BMC). **3**: Basalt small pillow/flow end with glass around (rounded edge). Bottom 3 mm glass, top 1 cm thick. Black-brownish grey, some parts are dark weathered. No clear vesicularity. Pl 3% (up to 3 mm). When dried, does not seem glassy anymore, maybe cracked basalt rather than glass. Extra rocks: 2 extra glassy basalts as **2** (extra 1, 2) 1 extra glassy basalt as **1** (extra 3) 1 basalt with large Pl phenocrysts (extra 4)
220 AUV Dive 103AUV Area N of The Batcave	71°13.464'/12°50.591'	20.07.12	655	no MAPR	Fresh basaltic glass sampled from nose AUV. Vehicle crashed into the wall with heading 290°
221 DR Thor's Hammer (clear volcanic cone) N NKR. W flank of the cone	71°20.839'/12°39.254' to 71°20.829'/12°38.631'	20.07.12 7:29 - 8:39	1272 – 1137	no MAPR	1 Basalt rock glass. **1**: 18x14x10 cm: Pillow basalt fragment with glassy rind, up to 4 mm thick. Glass is black with red palagonite. Basalt is reddish brown to gray, <1% vesicles (< 3 mm). No phenocrysts. **2xGl** (Kiel, BMC).
222 DR Thor's Hammer, N NKR, flat of the cone, up to the top.	71°20.820'/12°38.600' to 71°20.832'/12°37.755'	20.07.12 8:43 - 10:18	1139 – 1137	no MAPR	4 Basalt elongated pillow fragments, very fresh and no life. **1**: 16x10x6 cm (in 2 pieces): Elongated pillow with black glassy rind (1-4 mm), looks fresh, but oily. Dark gray basalt. No vesicles apart from ~5 mm thick zone (1 cm below the rim) with 30% vesicles (1-3 mm). Phenocrysts 2%, up to 2 mm: Pl +/- Ol? **2xGl** (Kiel, BMC). **2**: 9x7x5 cm: Elongated small pillow with black glassy rind. Similar as **1**, with 2 large (>1 cm) vesicles/holes. **2xGl** (Kiel, BMC). **2** to BMC Extra rocks: 2 extra basalts with glass rind, as **1**.
223 VSR Thor's hammer, on the flat cone. S most lava flow, E of fissure.	71°20.667'/12°37.900'	20.07.12 11:11 - 11:50	1138	no MAPR	Basaltic glass chips/fragments in all 7 cups. Cup 1 separate (contains large piece). Cups 2-7 together.
224 VSR Thor's hammer, on the flat cone. W of fissure at S side.	71°20.755'/12°38.204'	20.07.12 12:18 - 12:51	1139	no MAPR	Mud with basaltic glass chips/fragments in all 7 cups. All cups together. Separately also mud + glass collected from the base plate (potentially contaminated by previous VSR).
225 VSR Thor's hammer, on the flat cone. Centre of the cone.	71°20.808'/12°37.675'	20.07.12 13:16 - 13:58	1135	48 at 15 m	Basaltic glass chips/fragments in 3, 5, 7, with small amount of sediment. (others clean) All cups together.
226 VSR Thor's hammer, on the flat cone. N side, closer to the rim.	71°21.026'/12°37.784'	20.07.12 14:21 - 14:56	1142	no MAPR	Basaltic glass chips/fragments in 2, 3, 5, 6 with small amount of sediment. (others clean) Cups 2 and 5 together. Cup 3 and Cup 6 separate (larger pieces).
227 VSR Thor's hammer, on the flat cone. W side, higher flow close to the rim.	71°20.766'/12°38.516'	20.07.12 15:22 - 15:52	1140	no MAPR	Muddy small basaltic glass chips/fragments in 2 and 3 (+4) All cups together.

Station Area	Latitude (°N)/ Longitude (°W)	Date/ Time (UTC)	Depth (m)	MAPR nr.	Sample descriptions and samples taken (Gl = Glass; Pl = Plagioclase; Ol = Olivine; BMC = rock/glass to Bryn Mawr College, USA; Kiel = rock/glass to Geomar, Germany)
231 DR Hummocky terrain, N of Eggvin volcano (C NKR)	71°5.898'/12°51.086' to 71°5.729'/12°50.433'	22.07.12 8:02 - 9:10	592 – 528	48 at 250 m	¼ full with very big rock of thick basalt flows/pillows, some mud and sponges. **1**: 26x17x10 cm: Basalt flow, gray-brown-red. Glassy rind 1 mm to 1 cm thick with black areas underneath and palagonite outer crust. Vesicular throughout, 20-40% (1-3 mm). **2**: 13x12x10 cm: Basalt flow fragment with dark gray interior, ~45% vesicles (1-8 mm). Brown-red palagonite rind up to ~5 mm thick. No visible glass. **3**: 9x5x4 cm: Sheet flow fragment, dark gray with red. Rare large vesicles (>5 mm). Black glassy rind with palagonite outer surface (~1 cm thick for whole rind). **4**: 12x12x7 cm: Pillow fragment, brown to gray to black, with some red-orange alteration. ~30% vesicles (<1 mm – 4 mm). ~1 cm thick black glassy rind. **5**: a) 7x5x5 cm b) 6x4x4 cm c) 6x5x3.5 cm d) 7x5x3.5 cm e) 5x3.5x2.5 cm f) 5x5x4 cm: Small basalt flow fragments. Dark gray to brown interior, 20-30% vesicles (1-8 mm), black to red glassy rinds (<1 cm thick). **5a,b,d 2xGl** (Kiel, BMC). **5a, b, d** to BMC. Extra rocks: 4 extra basalts (with glass rind).
232 DR Clear sharp volcanic cone in rift valley N of Eggvins shoals volcano.	71°3.592'/12°57.139' to 71°3.393'/12°56.390'	22.07.12 10:07 - 11:25	622 – 578	48 at 300 m	¼ full with glassy basalt sheets/pillows. Fresh, some rusty alteration. **1**: a) 13x9x9 cm b) 14x9x5 cm c) 8x7x6 cm d) 8x6x4 ½ cm (freshest): Basalt sheet/pillow, subangular. Basalt dark grey, vesicular band of 10%, rest <2% (2-7 mm). Pl 1% (~2 mm). Glass crust up to 1 cm (fine crushed glass) on top. On bottom of **b**, large vesicular (2 cm), flow sink texture. Little palagonite on glass and rock (in bands). **1c 2xGl** (Kiel, BMC). **1c, d** to BMC. **2**: 14x10x8 cm: Basalt pillow. Dark grey rock. Glass rim (smooth) on top 1-4 mm thick. Red altered line, 1 cm under surface. Zones of vesicles, parallel to surface of 30%, rest ~1% (1-5 mm). Pl 1% (1 mm). **2xGl** (Kiel, BMC). **3**: a)19x15x8.5 cm b) 10x7x6 cm: Basalt flow with 2 mm – 1 cm glass. Zones of vesicles 20% (3-7 mm). Little red alteration under glass rim, but minor. Pl (1-2 mm) 1%. Lobate form for **a**. Vesicular/flow/sink texture on bottom (2 cm wholes). **4**: 14x13x11 cm: Basalt block. Top side very vesicular: 30%, bottom <1% (1-5 mm). Dark grey with orange alteration streaks. Pl 1% (1 mm). Extra rocks: 4 extra basalts as **1** (extra 1-4). 1 extra basalt as **2** (extra 5) 1 extra basalt as **3** (extra 6) 1 extra basalt as **4** (extra 7)
233 DR Small hummocks in flat rift valley, N of Eggvin shoals volcano	71°1.513'/12°57.517' to 71°1.329'/12°56.844'	22.07.12 12:21 - 13:17	673 – 627	48 at 250 m 50 at 300 m	~20 basalt pillow fragments. **1**: 33x24x18 cm: Pillow basalt, gray-brown-red colour. Moderately altered. 1-3 mm black glass, some red palagonite, fine grained. Flow textures on rind surface. 25% vesicles (1-6 mm). **2**: a) 15x10x9 cm b) 10x8x6 cm. Blocky basalt fragments. Gray with rusty streaks. 3 mm – 1 cm glass rind. Mostly black with a little palagonite. 5% vesicles in basalt (1-10 mm). **2a 2xGl** (Kiel, BMC). **2a** to BMC **3**: 13x11x9 cm: Basalt rock, 30% vesicles (1-10 mm). No glass. Black/brown colour, some yellowish alteration. **4**: 10x9x4 cm: Basalt rock, similar as **3**, with smaller vesicles (1-4 mm) 40% of the rock. **5**: 8x7x5 cm: Basalt rock, massive: <5% vesicles (1-2 mm, occasionally up to 1 cm). Orange palagonite alteration. Extra rocks: 4 extra basalts.

Station Area	Latitude (°N)/ Longitude (°W)	Date/ Time (UTC)	Depth (m)	MAPR nr.	Sample descriptions and samples taken (Gl = Glass; Pl = Plagioclase; Ol = Olivine; BMC = rock/glass to Bryn Mawr College, USA; Kiel = rock/glass to Geomar, Germany)
234 DR N hummocky flow of Eggvin volcano	70°59.343'/13°0.039' to 70°59.251'/12°59.196'	22.07.12 13:56 - 15:13	563 – 366	48 at 350 m	¼ full with semi-altered brown-black basalt with some thin glassy rims. (+ sealillies, sponges and yellow slime). **1**: a) 40x32x24 cm b)18x17x16 cm: Pillow basalt (fragment), brown altered. Vesicles (1-10 mm) 40%. At bottom up to 3 mm glass rim, on top 3-10 mm thick. Bottom surface pillow: imprint other pillow + flow structures. **2**: a) 12x12x10 cm b) 8x7x7 cm: Basalt pillow fragment, similar as 1, less altered. Vesicularity in zones 5-30% (1-10 mm). Dark grey-brown, some palagonite. Glass mostly black. **3**: 11x8x7 cm: Black to dark grey vesicular basalt (minor palagonite). 40-50% vesicles (1-10 mm). Minor palagonite. Glass on top? **4**: 12x8x8 cm: Vesicular basalt: 50% (3-10 mm) + one 4 cm pocket. Grey black to reddish brown. Flat, shiny surface on one side. Extra rocks: 2 extra basalts with glass rind, as **2**. 1 extra basalt as **4.**
235 DR S hummocky flow of Eggvin volcano.	70°54.765'/13°7.445' to 70°54.742'/13°6.749'	22.07.12 16:23 - 17:26	485 – 381	49 at 250 m	¼ full with pillow and flow basaltic fragments. **1**: a) 17x11x10 cm b) 15x9x6 cm: Basalt flow fragment. Dark gray. Mineral alteration. ~30% vesicles (1—10 mm). Black, fresh glassy rind (1 – 10 mm). **2xGl** (Kiel, BMC). **1a** to BMC. **2**: 22x18x14 cm: Pillow basalt, gray to brown interior with minor red alteration. ~20% vesicles (1-4 mm). Black glassy rind up to 7-8 mm with some red palagonite. **3**: 15x9x8 cm: Basalt fragment (flow interior?). Dark gray. 40% vesicles (2-10 mm). Relatively fresh. Extra rocks: 5 extra basalts with glass rind.
237 DR N edge of Southern Segment (S NKR), flat topped volcano in 'new' rift axis.	70°51.951'/13°37.296' to 70°51.742'/13°37.296'	23.07.12 8:03 - 9:30	1287 – ~1200	48 at 250 m	7 rock fragments. 6 glassy sheet basalt + 1 smooth basalt/dropstone? **1**: a) 15x11x6 cm: b) 10x8x4 cm: Basaltic sheet flow with glass on top (1 cm) and bottom (2 cm). Thick palagonite rim on outer surface (< 1 cm thick). Bottom: drip/vesicular/sink structures. Upper side flow structures. Interior glass fresh black. Basalt massive, gray <1% vesicles (1 mm). Pl phenocrysts 5% (up to a cm) in glass and basalt. **2**: 9x6x1 cm: Altered basalt/dropstone? Massive grey-brown-red basalt (?). Smooth weathered outer surface. No vesicles/crystals visible. Extra rocks: 2 extra basalts with glass rind as **1**.
238 DR Hummocks SW of volcano 237DR (S NKR).	70°50.722'/13°34.883' to 70°50.851'/13°34.229'	23.07.12 10:11 - 11:35	1402 – 1313	48 at 300 m	5 rocks of basalt pillow fragments. **1**: 27x23x20 cm: Basalt pillow/block. Brown-red-orange altered surface. Massive, no clear vesicles/minerals. Top glassy rind (2-3 mm thick), mostly palagonised, some black. **2**: 8x7x6 cm: Small pillow (fragment). Basalt yellow-orange-brown altered. No vesicles/crystals visible. Glass rind up to 5 mm thick with black glass (fresh) + ~60% palagonite. Glass all around the rock Extra rocks: 1 extra basalt with glass rind as **1** (extra 1) 2 extra basalts with glass rind as **2** (extra 2-3)
240 DR Small volcanic cone in southern transfer zone.	70°50.543'/13°23.827' to 70°50.788'/13°23.542'	23.07.12 16:08 - 17:35	1178 – 1016	48 at 250 m	8 basaltic pillow/flow fragments. **1**: 18x18x16 cm: Pillow basalt with <4 mm glass rind, partly (50%) palagonite. Gray interior. 3% Pl (<1 cm), some red alteration. 1-2% vesicles (<1 cm, irregular distributed). **2**: 7x6x5 cm: Basalt rock, grey. 10% vesicles (1-4 mm). No glass/minerals. **3**: 8x6x5 cm: Massive basalt, <1% vesicularity. No glass/minerals. Extra rocks: 1 extra basalts with glass rind as **1** 1 extra basalt as **2**

Station Area	Latitude (°N)/ Longitude (°W)	Date/ Time (UTC)	Depth (m)	MAPR nr.	Sample descriptions and samples taken (Gl = Glass; Pl = Plagioclase; Ol = Olivine; BMC = rock/glass to Bryn Mawr College, USA; Kiel = rock/glass to Geomar, Germany)
242 DR Hummocky terrain in the middle of the Easter valley in S NKR	70°45.598'/13°33.021' to 70°45.899'/13°32.690'	24.07.12 9:29 - 11:09	1559 – 1436	48 at 300 m	12 Basaltic pillows/sheet flows with (thick) glass rims, fresh. **1**: 23x17x15 cm: Pillow basalt, fresh top. Grey basalt, slightly brown-red altered. Vesicles <1%, apart from a 4 cm band from the top with 5% (1-8 mm). Glass crust on top of 1-7 mm thick, black (minor palagonite). 1% Pl (1 mm). **2**: a) 17x17x11 cm b) 13x8x7.5 cm c) 14x8x6 cm: Basalt sheet flows. Dark grey basalt. Glass on top (1 mm to 1 ½ cm thick). Smooth bottom (sink/flow structures) with some glass patches (up to a cm thick). **C** has thin (<2 mm) glass layer in between the rock. Vesicularity 5-10% (1 – 10 mm). Minor palagonite in the basalt, glass mostly fresh. No clear phenocrysts. **2b 2xGl** (Kiel, BMC). Extra rocks: 1 extra pillow basalt with glass rind as **1** 2 extra sheet basalts with glass rind as **2**
245 AUV Dive 105AUV E rift of S NKR	70°45.810'/13°34.133' Or 70°46.815'/13°31.530'	24.07.12	~1400	no MAPR	Fresh basaltic glass sampled from weight cavity AUV.
246 DR Hummocky flow N of 2 flat volcanoes in Western S NKR rift	70°47.365'/13°45.210' to 70°47.683'/13°45.240'	25.07.12 10:08 - 11:45	1714 – 1630	48 at 300 m	¼ full + 3 very big rocks stuck on top: Basaltic pillows/sheet flows with (thick) glass rims, fresh. **1**: 17x15x15 cm: Pillow basalt, glass all around, 1-4 mm thick. Fresh, some palagonite. Basalt, altered (palagonite: red-orange) outside, inside basalt fresher (grey brown). Vesicularity ~1% (1-2 mm). 2% Pl (up to 6 mm) in glass and in basalt. **2**: 15x12x10 cm: Similar to **1**, but fragment of pillow. Thicker glass layer up to 1 cm. Black, unaltered glass. **2b 2xGl** (Kiel, BMC). **3**: 46x38x12 cm (only ¼ taken): Sheet flow basalt. Smooth texture on one side, rough on the other side of the rock (grainy). Vesicularity 2% (1-2 mm). Grey to brown, reddish on some weathered surfaces. Inside fresh grey. 2% Pl (up to 1 cm); <1% Ol (up to 3 mm). Extra rocks: 1 extra pillow basalt with glass rind as **1** 2 extra pillow fragment basalts with glass rind as **2**
247 DR Hummocky volcano at SE side of eastern valley S NKR	70°39.475'/13°37.165' to 70°39.749'/13°37.226'	25.07.12 14:02 - 15:50	2064 – 1972	48 at 250 m	Some mud (clumps), no rocks.
248 DR Hummocky ridge on east flank of S NKR	70°44.676'/13°27.878' to 70°44.962'/13°27.949'	25.07.12 16:40 - 18:21	1658 – 1511	48 at 300 m	¼ full (incl. Big rock) with semifresh glassy pillow basalt fragments. Some life. **1**: 23x23x14 cm: Pillow basalt. Outside fairly altered with orange/yellow/gray/white alteration colours. Glass rind on top < 1.5 cm thick, also variably altered from black to red-orange palagonite. Vesicles 2% (1-8 mm). <1% phenocrysts (Pl?) **2**: 14x10x7 cm: Pillow basalt fragment, same as **1**, with strong yellow-orange-green alteration. **3**: 17x8x7 cm: Pillow basalt, gray, 2 mm glass on top with strong red palagonite alteration. 5% vesicles (1-8 mm); 2% Ol phenocrysts (<3 mm). Extra rocks: 1 extra pillow fragment basalt with glass rind as **1** 2 extra pillow fragment basalts with glass rind as **3**
250 DR Sheetflows in sidescan at N end of S NKR (reflective). N one of the two flows.	70°54.535'/13°32.374' to 70°54.268'/13°32.436'	26.07.12 8:00 - 9:21	1165 – 1198	48 at 250 m 50 at 300 m	Empty
251 DR Same as 250DR	70°54.546'/13°32.382' to 70°54.236'/13°32.866'	26.07.12 9:34 - 11:05	1180 – 1192	No MAPR	Empty
252 DR Sheetflows in sidescan at N end of S NKR (reflective). S one of the two flows.	70°52.958'/13°31.772' to 70°52.563'/13°32.763'	26.07.12 11:24 - 13:27	1321 – 1400	48 at 350 m	Empty

Station Area	Latitude (°N)/ Longitude (°W)	Date/ Time (UTC)	Depth (m)	MAPR nr.	Sample descriptions and samples taken (Gl = Glass; Pl = Plagioclase; Ol = Olivine; BMC = rock/glass to Bryn Mawr College, USA; Kiel = rock/glass to Geomar, Germany)
253 DR Crater of Eggvin volcano. Over small hummocky hills.	70°56.938'/13°2.085' to 70°56.845'/13°2.262'	26.07.12 16:57 - 17:32	207 – 175	48 at 10 m 50 at 40 m (in separate drop down)	¾ full of rocks: fresh, popping, very vesicular, fragile basalt pillows/sheetflows **1**: 20x16x14 cm: Black fresh, popping pillow basalt. Variety of flow textures (e.g. pillow head, a-a type, more ropy), ranges from massive (5% vesicles, 2 mm) to vesicular (40%, 1 mm); Glassy areas (1-5 mm) on several of the flow texture. **2**: 17x17x10 cm: Similar to **1**, but more sheet basalt like (2 surfaces) more massive and altered. Less friable, layered textures and ~1 cm glass rinds. Some mildly altered areas. Vesicularity ranges from 0-25% (<1 mm). **3**: 13x9x7 cm: Similar to **1**, with thick massive rock areas (5% vesicles, <1 mm) and minor glassy vesicular areas (40%, 1-2 mm). Less flow textures. **4**: 14x13x10 cm: Similar to **1**. Crusty glass texture (a-a like), 10% vesicles (< 1 mm). Fragile. **5**: 6x5x4 cm: Similar to **1**, with ropy, stingy flow texture. **6**: 13x12x10 cm: Similar to **2**. With ~1 cm glass rinds. Relatively massive interior with massive interior with ~10% vesicles (1-3 mm elongate vesicles and 4 mm gas pockets). Slightly altered. **6** to BMC. Extra rocks: 6 extra fresh, popping pillow/sheet basalt rocks.
255 VSR Sheetflows in sidescan (reflective) at N end of S NKR. S one of the two flows.	70°52.857'/13°32.175'	27.07.12 10:55 - 11:42	1357	no MAPR	Basaltic glass chips/fragments in 4 and 7. All cups together.
256 DR Small (30 m) hummocks in (potentially not hitted) in flat rift valley floor. N of Eggvin volcano C NKR	71°6.797'/12°55.218' to 71°7.094'/12°55.135'	27.07.12 13:49 - 15:07	730 – 721	48 at 300 m	Full with mud.
257 DR Hummocky basalt flow in AUV side scan, E of Batcave C NKR	71°12.892'/12°47.247' to 71°13.987'/12°47.208'	27.07.12 16:12 - 17:21	624 – 644	48 at 300 m	1 Basalt fragment **1**: 15x10x9 cm: Dark gray basalt, flow fragment. 15% vesicles (1-4 mm), relatively fresh with minor alteration. 4 mm glass rind (in one corner) with fresh black glass, underneath a brown weathered outer surface.
260 DR Sheet flow in northern AUV sidescan area (N of Thor's Hammer). Flat flow, moderately reflective in sidescan. N NKR.	71°24.222'/12°32.718' to 71°23.685'/12°32.647'	28.07.12 8:29 - 10:32	1580 – 1559	No MAPR	3 rocks of basalt flows and pillow. **1**: 17x15x15 cm: Brown to dark gray pillow basalt fragment with 1-2 mm glass rind, mostly palagonised. 5% vesicles (< 1 cm) and moderately altered. **2**: 17x10x10 cm: Dark grey sheet (?) flow, with palagonite and glass rind on two surfaces (2 mm at bottom, 5 mm at top). Flow textures on top surface. Interior basalt relatively fresh, 5% vesicles (1-2 mm). **3**: 8x7x5 cm: Basaltic glass sheet flow. With <1 mm palagonite, on the surfaces. Rest of the glass fresh. Large voids inside (up to 2 cm); ~1% Pl (2 mm phenocrysts). Flowing textures.
261 DR E of spreading axis.	71°24.222'/12°32.718' to 71°23.685'/12°32.647'	28.07.12 8:29 - 10:32	1580 – 1559	48 at 300 m moved to 230 m when up	Empty, dredge completely entangled.

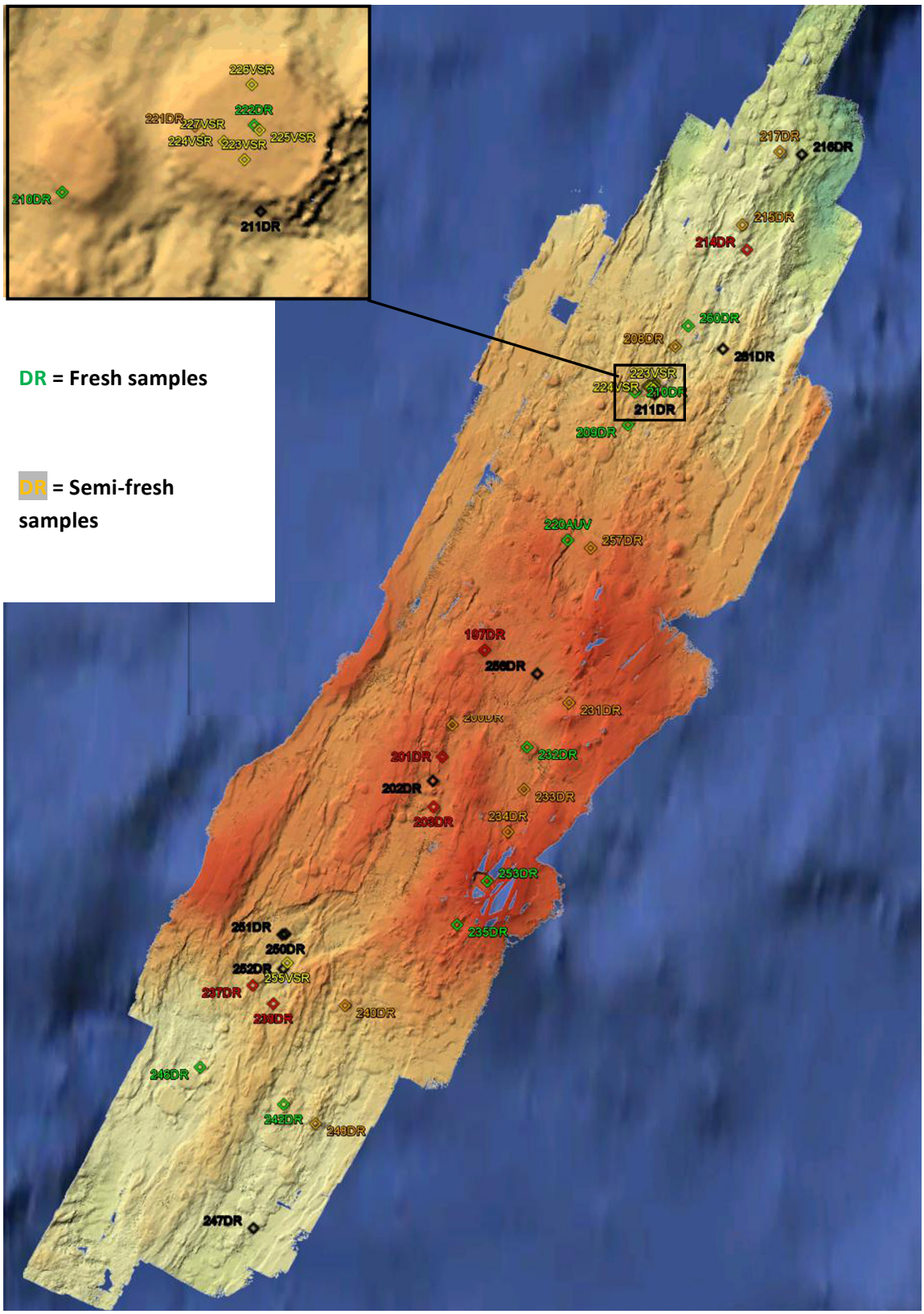

Figure 9.1: Overview of Samples locations

10 Literature

Baker, E. T., and H. B. Millburn (1997), Mapr: A new instrument for hydrothermal plume mapping, *Ridge Events*, *8*(1), 23-25.

Blichert-Toft, J., A. Agranier, M. Andres, R. Kingsley, J.-G. Schilling, and F. Albarède (2005), Geochemical segmentation of the mid-atlantic ridge north of iceland and ridge–hot spot interaction in the north atlantic, *Geochem. Geophys. Geosys.*, *6*(1), 27.

Haase, K. M., C. W. Devey, and M. Wienecke (2003), Magmatic processes and mantle heterogeneity beneath the slow-spreading northern kolbeinsey ridge segment, north atlantic, *Contrib. Mineral. Petrol.*, *144*, 428-448.

Hooft, E. E. E., B. Brandsdottir, R. Mjelde, H. Shimamura, and Y. Murai (2006), Asymmetric plume-ridge interaction around iceland: The kolbeinsey ridge iceland seismic experiment, *Geochem. Geophys. Geosyst.*, *7*, Q05015.

Kodaira, S., R. Mjelde, K. Gunnarsson, H. Shiobara, and Shimamura (1997), Crustal structure of the kolbeinsey ridge, north atlantic, obtained by use of ocean bottom seismographs, *J. Geophys. Res.*, *102*, 3131-3151.

Mertz, D. F., W. D. Sharp, and K. M. Haase (2004), Volcanism on the eggvin bank (central norvegian-greenland sea, latitude ~71°n): Age, source, and relationshipto the iceland and putative jan mayen plumes, *Journal of Geodynamics*, *38*, 57-83.

Mjelde, R., J. I. Faleide, A. J. Breivik, and T. Raum (2009), Lower crustal composition and crustal lineaments on the voring margin, ne atlantic: A review, *Tectonophysics*, *472*(1-4), 183-193.

Mjelde, R., A. J. Breivik, T. Raum, E. Mittelstaedt, G. Ito, and J. I. Faleide (2008), Magmatic and tectonic evolution of the north atlantic, in *Journal of the Geological Society*, edited, pp. 31-42.

Schilling, J., R. Kingsley, D. Fontignie, R. Poreda, and S. Xue (1999), Dispersion of the jan mayen and iceland mantle plumes in the arctic: A he-pb-nd-sr isotope tracer study of basalts from the kolbeinsey, mohns, and knipovich ridges, *J Geophys Res-Sol Ea*, *104*(5), 10543-10569.

Smith, D. K., S. Humphris, and W. B. Bryan (1995a), A comparison of volcanic edifices at the reykjanes ridge and the mid-atlantic ridge at 24-30°n, *J. Geophy. Res.*, *100*, 22485-22498.

Smith, D. K., et al. (1995b), Mid-atlantic ridge volcanism from deep-towed side-scan sonar images, 25-29°n, *J. Volcanol. Geotherm. Res.*, *67*, 233-262.